KINETIC ANALYSIS OF ENDOSOME PROCESSING: MATURATION OF EARLY ENDOSOMES AND VESICULAR TRAFFIC TO LYSOSOMES

Thesis presented by

EVELYN JOY STROUD

in fulfilment of the requirement for the degree of

Master of Science

in

Medical Sciences (Medical Biochemistry)

in the

Faculty of Medicine

University of Cape Town

Supervisor: Prof. Lutz Thilo

February 1995

SUMMARY

The present study was undertaken to establish the mechanism(s) involved in the endocytic pathway, in particular, early endosome processing and delivery to the lysosomes. Two models for endosome processing have previously been proposed in the literature, namely the maturation and vesicular traffic models. The general consensus has been an early phase of intermingling of the endocytic contents markers within early endosomes that mature to form non-fusogenic late endosomes (maturation model). This maturation phase is followed by a segregation phase where intermingling of contents between vesicles no longer takes place.

To establish the mechanism(s) involved in early endosome processing and delivery to lysosomes, a kinetic analysis was made using results from cellular fluid-phase uptake assays. This unique approach offers an alternative view to previous studies on the mechanisms in operation during endocytic processing. The results and conclusions made could thus confirm or disprove previously proposed mechanisms.

A mouse macrophage cell line, $P388D_1$, was used together with fluoresceine isothiocyanate-dextran (FITC-D) and horse radish peroxidase (HRP) as fluid phase markers. The HRP-mediated 3,3'-diaminobenzidine (DAB)-crosslinking technique

was applied to intact cells and FITC-D was found to be fully susceptible to the cross-linking by DAB when FITC-D colocalized with HRP. When FITC-D and HRP were endocytosed sequentially, the proportion of endocytosed FITC-D not associated with HRP was measured as the percentage soluble FITC-D. The percentage of soluble FITC-D is a measure of the extent of intermingling of the sequentially endocytosed fluid phase markers. From the resulting FITC-D solubility profiles a kinetic analysis could be made to indicate the involvement of either a maturation or vesicular process. A sigmoidal shaped curve for the segregation of endocytic contents would be indicative for a maturation process (having zero-order kinetics), while vesicular trafficking (a process involving first-order kinetics) would not allow for full segregation.

The kinetics of intermingling of the two fluid-phase markers in this study showed that during early endocytic processing of sequentially endocytosed ligands a decrease in intermingling of the ligands was observed. This could be explained by a maturation of the early endosomes to become late non-fusogenic endosomes. The average maturation period of an endosome, at 37°C, was found to be approximately 3 min.

The later part of the endocytic pathway was investigated to determine whether the maturation model was consistent

with the kinetics of the delivery of endocytic contents to lysosomes. Firstly a direct approach was based on separating endosomes from the more dense lysosomes using a percoll gradient. Endocytosed marker was found to accumulate in lysosomes with first order kinetics, $T_{\frac{1}{2}} \approx 5.5$ min. In the second (indirect) approach the kinetics of intermingling of sequentially endocytosed markers in the lysosomal compartment were determined. Intermingling at late endosomal-lysosomal stages occurred with a first order kinetics, indicating that endocytosed ligand was delivered to lysosomes by vesicular traffic.

A number of control experiments were performed using conditions that effect processing along the endocytic pathway. Lysosomal delivery is delayed at low temperatures. Accordingly, results in this study show that at 16°C the rate of endocytic processing decreased and lysosomal delivery was only observed after ≈ 6h.

Similarly, a Na^+-depleted buffer has previously been shown to inhibit lysosomal delivery. A Na^+-depleted buffer was used in this study as a control for the absence of lysosomal delivery. It was found that the presence of a Na^+-depleted buffer resulted in a decrease in the lysosomal buoyant density. Contrary to previous assumptions, HRP delivery took place in the presence of a Na^+-depleted buffer, albeit at a slower rate than when in the presence of a Na^+-containing

buffer. Na^+ depletion appears to have a physiological effect on both the lysosomal buoyant density and the rate at which endocytic processing can occur.

The drug Brefeldin A (BFA) links up compartments of the endocytic pathway. Preliminary experiments were done to determine the effect of BFA on the fluid-phase uptake rate by cells. The rate of fluid-phase endocytosis was decreased but cells regained their endocytic rate after BFA had been withdrawn from the medium. Further studies in the presence of BFA may show different kinetics for intermingling of endocytic contents.

Essentially this study provides evidence for the involvement of a maturation process during early endosome processing followed by vesicular traffic for the delivery of ligand to lysosomes.

ACKNOWLEDGEMENTS

I would like to express my thanks and appreciation to:

Prof. Lutz Thilo for your supervision

Dr. Tom Haylett for all your help and guidance in the laboratory

Also to my colleague, Henk Tandt, for your assistance and help with the upkeep of our cell cultures

To all the staff working in this department

The Foundation for Research and Development for their funding.

CONTENTS

INDEX TO FIGURE TITLES

INTRODUCTION

Although early and late endosomes, as well as lysosomes, are well established stages of endocytosis, many aspects of trafficking along the endocytic pathway remain poorly understood and controversial. The objective of this thesis will be an attempt to help determine whether endocytic processing occurs by vesicular traffic or by maturation, specifically with regard to early endosome ligand processing and the delivery of ligand from late endosomes to lysosomes. An understanding of the fundamental processes occurring within a cell is crucial for the establishment of a secure framework from which research can be developed.

To set the scene, I will start by giving an overview of the endocytic pathway and the organelles involved with the endocytic process. This will be followed by the models previously proposed and the research undertaken in this field and finally, the approach taken for this particular study.

(i) The endocytic pathway

The endocytic pathway occurs in all eukaryotic cells and essentially involves the uptake of molecules from their surrounding medium by endocytosis, followed by the transportation and delivery to various destinations within a

cell. Endocytosis is said to occur either by fluid-phase or by receptor-mediated endocytosis. Receptor-mediated endocytosis occurs when ligands bind to receptors found within a clathrin coated pit (Pearse and Bretscher, 1981) which will invaginate and pinch off to form a coated vesicle (Silverstein *et al.*, 1977). Removal of the coat by an Adenosine 5'-triphosphate (ATP)-dependent enzyme (Schlossman *et al.*, 1984) gives rise to an uncoated fusogenic vesicle. The receptors are recycled to the plasma membrane after dissociation from their ligands, induced by the low pH environment. Molecules that do not bind to the plasma membrane, while being endocytosed, are said to be taken up in pinocytic vesicles by fluid-phase endocytosis (Steinman *et al.*, 1983). Both receptor and fluid-phase endocytosed material are transported at the same rate along a common endocytic pathway (Ward *et al.*, 1989). Following internalization, the molecules are transported within a vesicle along the endocytic pathway to specific target sites by fusion of the vesicles.

Numerous morphological and biochemical studies have in the past been undertaken to elucidate the process of endocytosis (Murphy, 1985; Stoorvogel *et al.*, 1991; Gruenberg and Howell, 1986 and 1987; Salzman and Maxfield, 1988 and Dunn and Maxfield, 1992 for example). The mechanisms involved whereby endocytosed material is transferred to endosomes and then to lysosomes and other destinations within the cell are

unclear. It is accepted that endosome processing can either occur by maturation of the vesicles or by vesicular trafficking at a particular site along the endocytic pathway. The following schematic diagram outlines the endocytic pathway and the insets represent the two proposed models, (1): vesicular traffic and (2) maturation.

A SCHEMATIC DIAGRAM SHOWING THE ENDOCYTIC PATHWAY

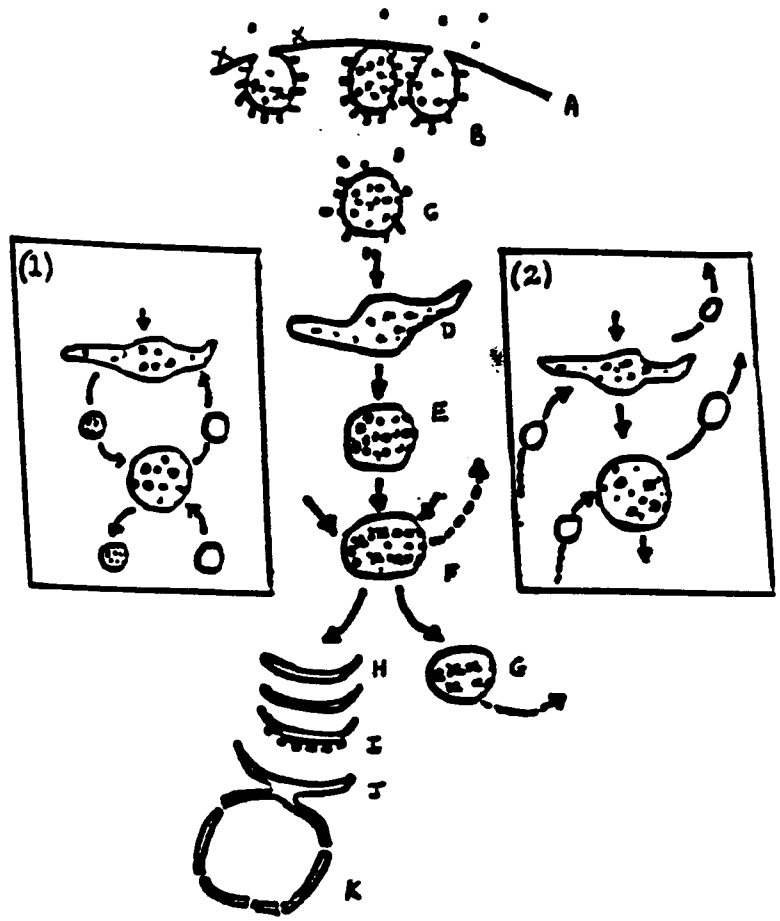

A: Plasma membrane where ligands (●) are unbound (fluid-phase uptake), B: Coated pit, C: Coated vesicle, D: Early endosome, E: Multivesicular body (Late endosome), F: Prelysosomal compartment (accumulation and sorting of ligands and possible recycling), G: Secondary lysosome. H: Golgi cisternae, I: Rough Endoplasmic Reticulum (RER), J: Endoplasmic Reticulum (ER) and K: Nucleus

The initial stage of the endocytic pathway involves the rapid internalization of the molecules/ligands into small endocytic vesicles. Ligands are next found in larger tubulo-vesicular sorting early endosomes where sorting of the receptors and lysosomally targeted ligands takes place. These ligands are then delivered to the late endosomes which are well distinguished from sorting endosomes as they contain low amounts of most recycling receptors. Geuze *et al.* 1983, have shown that endosomes are associated with tubules which may either become, or empty into, recycling vehicles able to transport their contents back to the cell surface. These `endosomal' structures have been termed the compartment for uncoupling of receptor and ligand (CURL). Ligands that are not to be degraded in lysosomes may also be transported to the Golgi/ER apparatus for cell regulatory and processing activities.

(ii) Organellar components of the endocytic pathway

The endocytic pathway comprises two major compartments, namely the endosomes and the lysosomes. The endosomes are organelles which receive the ligands and fluid internalized by the cell and the lysosomes are the degradative acid hydrolase-rich organelles.

Endosomes were first described by Straus in 1964 and have been found to play an essential role in the sorting,

segregation and addressing of all internalized constituents. They consist of a heterogeneous population of often irregularly shaped, electron-lucent vacuoles located at the periphery of the cytoplasm or in the perinuclear region (Wall *et al.*, 1980; Geuze *et al.*, 1983; Hopkins and Trowbridge, 1983; Marsh *et al.*, 1986 and Gruenberg and Howell, 1987). Endosomes have a lower buoyant density than secondary lysosomes (Tolleshaug *et al.*, 1979) and their protein composition is very similar to that of the plasma membrane (Mellman *et al.*, 1980 and Marsh *et al.*, 1983). The major physiological activity reported for endosomes is the ATP-dependent acidification process (Gruenberg and Howell, 1986).

The endosome compartment can be divided into two functionally distinct sub-compartments, namely, the early and late endosomes (Wall and Hubbard, 1984; Mueller and Hubbard, 1986; Murphy 1985; Gruenberg and Howell 1986, 1987 and 1989; Schmid *et al.*, 1988 and Gruenberg *et al.*, 1989). The early endosomes receive all components internalized from the cell surface, and is the major site for sorting and recycling of the receptors back to the plasma membrane. The second compartment comprises the late endosome, which has been described as a multivesicular structure (Gruenberg and Howell, 1989). In essence, late organelles function both to receive material from the early endosomes and to deliver their contents into the lysosomes.

A mechanism by which endosomes and / or lysosomes increase their density could be the result of a low pH induced aggregation of vesicle contents, thereby decreasing the osmotic pressure inside the vesicle (Roederer *et al.*, 1987). This is a useful feature which allows one to separate the early endosomes from the lysosomes (by using a percoll gradient, for example). Lysosomes are generally classified as either a primary or secondary lysosome. A primary lysosome contains acid hydrolases formed by the RER and Golgi apparatus. The secondary lysosome, also an acid hydrolase rich vacuole, acquires substrates by endocytosis (Steinman *et al.*, 1983 and Geuze *et al.*, 1988).

(iii) Models previously proposed for endocytic processing

Currently three models are accepted to describe the organellar mechanism(s) which govern transfer along the endocytic pathway. These being: (a) the vesicular traffic model; (b) the maturation model and (c) the endosomal network model.

(a) Vesicular traffic model, originally proposed by Palade (1975), predicts that early and late endosomes as well as lysosomes are preexisting organelles. Communication between these organelles occurs via carrier vesicles that bud from one compartment to the next delivering their membrane and

content by fusion and then recycle, thus allowing transportation and delivery along the endocytic pathway. Early and late endosomes are therefore assumed to contain resident proteins in addition to the molecules in transit. Support for the endosome vesicular model is given by both Gruenberg *et al.* (1989) and Griffiths and Gruenberg (1991)

(b) The maturation model implies that early endosomes will constantly be formed by the fusion of incoming vesicles with one another. This early endosome matures while being translocated in the cell to become a late endosome and eventually a lysosome.

(c) The more recent endosomal-network model is based on the observation made by Hopkins *et al.* (1990) that endocytosed markers enter a network of tubular cisternae containing discrete swellings analogous to the vesicular endosomal compartment. Communication within these tubules are mediated by a unidirectional movement along the tubules. Tubular endosomes have been found to occur in cells of many lines (Tooze and Hollinshead, 1991), the extent of tubular endosomes varying greatly between different cell types. Stoorvogel *et al.* (1991) detected long tubular extensions of endosomes in various cell types and proposed the possible presence of connections between early and late endosomes via tubular extensions. Whether endosomes assume a tubular morphology in all cells is not clear in view of the difficulties encountered for preserving and detecting these fragile structures. Therefore, for the purpose of this study

only the maturation and vesicular traffic models are debated.

(iv) General overview relating to endocytic processing events previously studied

Support for the maturation model is based on the loss of fusogenicity of the early endosomes and the consequent segregation of contents while a subcellular distribution of characteristic markers (eg. existence of GTP-specific binding proteins) suggests the presence of '*compartment-specific machinery*' (Griffiths and Gruenberg, 1991) thus giving support for the vesicular traffic model.

De Duve and Wattiaux (1966) initially proposed that fusion events among endocytic vesicles mediate the transfer of internalized material from one endocytic compartment to another. Several cell-free assay systems have been developed to study fusion amongst endosomes (Davey *et al.*, 1985; Gruenberg and Howell, 1986; Braell, 1987; Gruenberg *et al.*, 1989; Woodman and Warren, 1988 and Diaz *et al.*, 1988. Further studies by Gruenberg and Howell (1987) found that fusion competence was at a maximum from fractions isolated 5 min after internalization and decreased with a $T_{\frac{1}{2}} \approx 3$ min for fractions isolated at later time points. Similarly, Ajioka and Kaplan (1986); Salzman and Maxfield (1988); Ward *et al.* (1990) and Dunn and Maxfield (1992) showed that early

endosomes, containing sequentially endocytosed markers, intermingled their contents but that the efficiency of intermingling decreased rapidly following an increased interval between the uptake of the two ligands. Their results suggested that the vesicle fusions occur during a brief time window in which pre-existing endosomes can fuse with newly formed endocytic vesicles. These early endosomes then mature to a state where they are no longer fusogenic with newly internalized vesicles. Salzman and Maxfield (1989) established that fusion continued for 5 - 10 min after the initial internalization of the ligand into the cell and that the $T_{\frac{1}{2}}$ for the loss of fusion accessibility was ≈ 8 min. Dunn and Maxfield (1992) studied the properties of individual endosomes and showed that a pulse of ligand was retained by individual sorting endosomes, arguing that for a vesicular model the concentration of ligand in early endosomes would decline during the chase interval. They also argued that the loss of fusogenicity by early endosomes does not comply with a vesicular process as early endosomes should continue to receive newly endocytosed ligands, which was not found to be so.

Support for the vesicular traffic model by Merion and Sly (1983) was based on the observation that internalized ligands were delivered to structures of intermediate density before delivery to the lysosomes. Endocytosed ligands are therefore assumed to be delivered in vesicles to pre-

existing compartments and not within the same vesicle which matures to become a late endosome. Murphy (1985) also suggested that intermediate vesicles were labeled by fusion with the small primary endocytic vesicles. Gruenberg *et al.* (1989) observed, using *in vitro* and *in vivo* biochemical and morphological experiments, the transport of spherical vesicles between early and late endosomes and found that the process required intact microtubules. Later, Griffiths and Gruenberg (1991) argued that early and late endosomes were pre-existing organelles rather than transient vesicles undergoing a maturation process.

Delivery of an endocytosed ligand from the late endosomes to the lysosomes has been addressed in the literature on a smaller scale when compared to the early stages of endocytosis. Evidence supporting a maturation process was given by Stoorvogel *et al.* (1991), Storrie *et al.* (1984) and Roederer *et al.* (1987 and 1990). Storrie *et al.* (1984) used HRP to study the process by which pinosome contents are delivered to lysosomes. Progressive vesicle processing for the delivery of an endocytosed ligand was found to occur in two stages, namely: delivery to a prelysosomal and lysosomal stage which took 6 - 10 min and 1 h respectively. Roederer *et al.* (1987 and 1990) observed that isolated endosomes could undergo an increase in density *in vitro* to that of lysosomes and concluded that this mimics the density change which occurs *in vivo*. Stoorvogel et al. (1991) argued in

favour of early endosomes maturing all the way to prelysosomal organelles based on their observation that labeled transferrin was seen at gradually increasing densities on density gradients.

Control experiments using either low temperature, a Na^+-depleted buffer or Brefeldin A (BFA) were performed to affect processing along the endocytic pathway. The effect of low temperature on endosome-lysosome fusion has previously been investigated (Dunn *et al.*, 1980; Stoscheck and Carpenter, 1984; Hopkins and Trowbridge, 1983; Pesonen *et al.*, 1984 and Roederer *et al.* 1987 and 1990). It was presumed that delivery to lysosomes was inhibited at temperatures below 20°C. Haylett and Thilo (1991) showed that at 16°C endosome-lysosome fusion did occur but after approximately 6h of incubation. Similar experiments were performed to verify these results and to observe the effect of low temperature on experiments undertaken in this study.

Na^+-depleted was found to inhibit the delivery of a ligand to the lysosomes (Wolkoff *et al.*, 1984 and Ward *et al.*, 1990) and was therefore used in this study as a control.

BFA has been shown to have profound effects on the morphology of various compartments of the endosome-lysosome system (Klausner *et al.*, 1992 and Wood and Brown, 1992). BFA should be a useful means to investigate intermingling and

delivery at various stages of the endocytic pathway as it may show different kinetics for intermingling of endocytic contents.

(v) Experimental approach

The principle aim of this study was to establish the mechanism(s) involved during early endocytic processing and during the delivery of the ligands to the lysosomal compartments in a macrophage cell line, $P388D_1$. In addition, delivery to lysosomes at low temperature (27/16°C) was investigated as well as the effects of a Na^+-depleted buffer and BFA on the endocytic pathway.

Different experimental approaches have previously been undertaken to investigate which endocytic model applies to the endocytic pathway, for example: flow cytometry (Murphy 1985); cell homogenization (Stoorvogel *et al.*, 1991); immunoisolation (Gruenberg and Howell, 1986 and 1987) and digital image analysis using specialized equipment (Dunn and Maxfield, 1992).

A fundamental aspect of the above studies consisted of measuring intermingling of two fluid-phase markers after sequential internalization. Intermingling is determined in terms of intraorganellar colocalization of two different endocytosed ligands. Both the maturation and vesicular

models involve numerous fusion events which lead to intermingling of the endocytosed ligands. The two models, however, imply distinct kinetics for the degree of intermingling at various times after endocytic uptake. The vesicular traffic model would lead to an almost immediate appearance of ligand at various stages along the pathway (first-order kinetics). A maturation process will lead to a progressive processing with ligand arriving in each successive compartment only after each respective maturation period (zero-order kinetics).

In this study, the quantitative and kinetic aspects of intermingling of sequentially endocytosed fluid-phase markers were analyzed. FITC-D and HRP were used as fluid phase markers and their intermingling was studied by observing colocalization as based on HRP-mediated DAB-crosslinking. FITC-D was fully susceptible to crosslinking of DAB when it colocalized fully with HRP as during simultaneous endocytic uptake. When sequential uptake of the two markers resulted in only partial colocalization of FITC-D with HRP in the same organelles (intermingling), the fraction of FITC-D in HRP-free organelles remained detergent soluble after HRP-mediated DAB crosslinking. By measuring the fluorescence intensity in detergent soluble fractions the relative amount of non-colocalizing FITC-D could be quantitated. These values were plotted as a function of time which separated the two uptake pulses.

Intermingling of sequentially endocytosed FITC-D and HRP due to common delivery to lysosomes, or due to fusion between lysosomes, was measured by chasing the endocytic pulses towards late stages of the endocytic pathway. Lysosomal delivery was also studied directly, by cell fractionation which allowed the isolation of high density lysosomes on Percoll density gradients.

CHAPTER 1

PRELIMINARY EXPERIMENTS

1.1 HRP AND FITC-D AS MARKERS FOR FLUID-PHASE ENDOCYTIC UPTAKE

Both FITC-D and HRP have previously been used as fluid-phase markers in a variety of cells (eg. Storrie *et al.*, 1984 and Steinman and Cohn, 1972). Studies by Wileman *et al.* (1986) showed that HRP, as a mannose bearing molecule, binds to the macrophage mannose receptor. Although $P388D_1$ cells are known to only have a few mannose receptors (Stahl and Gordon, 1982), mannan (1 mg/ml) was nevertheless included in the medium on all occasions when using HRP to ensure that only fluid-phase uptake occurs. In order to test the fluid-phase markers for their suitability in the present study, an experiment as outlined in FIG. 1.1.1 was performed.

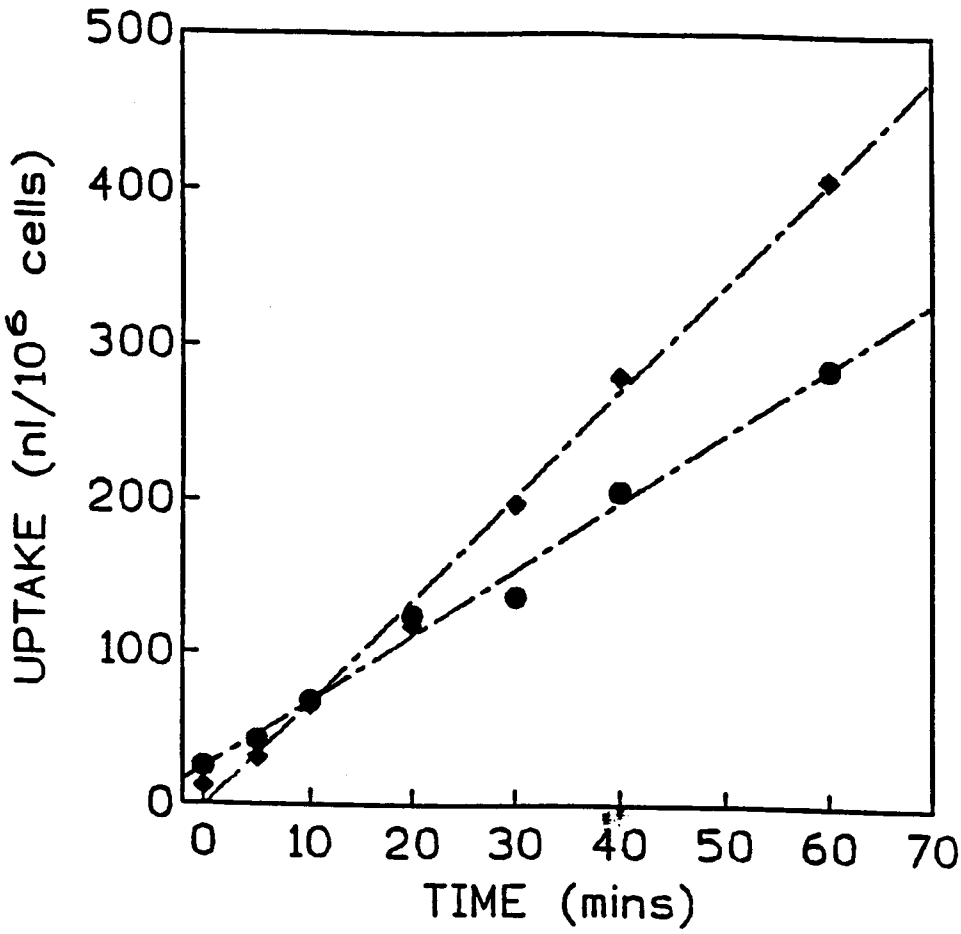

FIG. 1.1.1 FLUID-PHASE UPTAKE ASSAY USING FITC-D AND HRP

Cells were incubated at 37°C either in the presence of FITC-D (2 mg/ml, ♦) or HRP (1 mg/ml, ●) as fluid-phase markers. At the indicated times, uptake was stopped by cooling on ice, external marker removed by washing, and cell associated marker measured and normalized to cell number. Conversion to volume of uptake, as indicated, was done by using a standard curve (not shown). The data points refer to the average obtained from duplicate samples in a single experiment. The 'best-fit' straight lines are for 6.7 (♦) and 4.4 (●) $nl/10^6$ cells.min.

The result shows that uptake occurred linearly with time over a period of 60 min. This suggested that loss of endocytosed marker from the cells was negligible (cf. FIG 1.1.2 below). Ideally behaving fluid-phase markers should indicate identical values for fluid-phase uptake. However, the present results indicated a higher fluid-phase uptake rate for FITC-D (6.7 nl/(10^6cells.min)) as compared to when HRP was used (4.4 nl/(10^6cells.min)). The reason for this is unknown, but similar results were found previously (Begg, M. J., 1992). This was probably the result of the normally observed variation between independent experiments, as was found when using the same marker on various occasions (results not shown). This problem could have been addressed by incubating the cells in the presence of both ligands simultaneously. For the present study, however, only relative values for fluid-phase uptake were required.

Subsequent experiments were to involve the uptake of HRP and FITC-D followed by extended periods of incubation in marker free medium (chase period). It was therefore essential to establish that previously endocytosed marker was not lost from the cells. Therefore, we directly tested whether endocytosed fluid phase marker remained in the cell for the duration of an anticipated experiment. The extent of release of the marker is shown in FIG. 1.1.2.

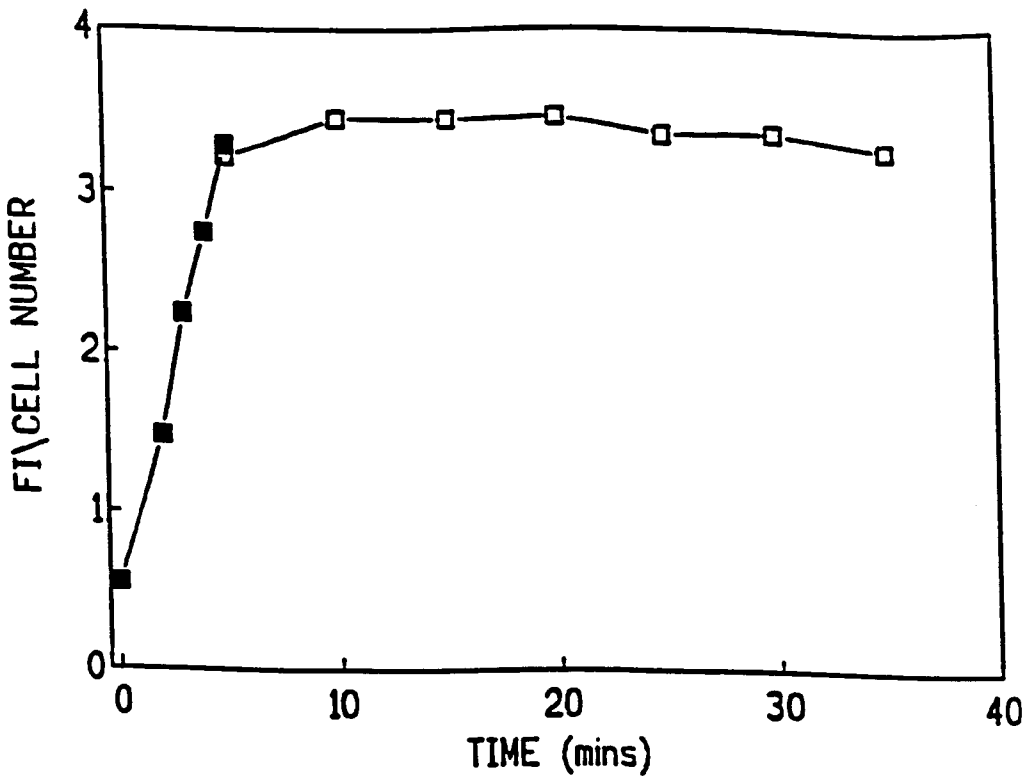

FIG. 1.1.2 STABILITY OF FITC-D IN MACROPHAGE CELLS

Cells were incubated at 37°C in the presence of FITC-D (3mg/ml), allowing fluid-phase uptake (■,cf. FIG 1.1.1). At 5 min, cells were placed on ice to temporarily halt uptake and washed to remove non-internalized ligand. During incubation in FITC-D free-medium, samples were taken at the indicated time points by cooling on ice (□). Cell associated FITC-D was determined (Fluorescent intensity, FI, see methods) and related to cell number, as indicated.

The results show that in the absence of external FITC-D, cell associated marker remained constant over a period of 30 min, as investigated. Therefore, no significant loss of marker by retro-endocytosis occurs. A similar observation has been made for HRP in macrophage cells by Swanson *et al.*

(1985). Fluid-phase marker was maintained sufficiently stable in cells to allow subsequent experiments involving extended chase periods.

1.2 EFFICIENCY OF FITC-D CROSSLINKING WITH DAB IN WHOLE CELLS AS A FUNCTION OF HRP CONCENTRATION

The reason for using HRP as one of the fluid-phase markers is based on its ability to mediate DAB crosslinking in HRP containing organelles. If FITC-D in an organelle containing HRP is effectively trapped by DAB-crosslinking it will become detergent insoluble. To establish the concentration range of HRP which would be required to cause maximal FITC-D trapping by DAB crosslinking, the following experiment was undertaken, cf. FIG. 1.2.1.

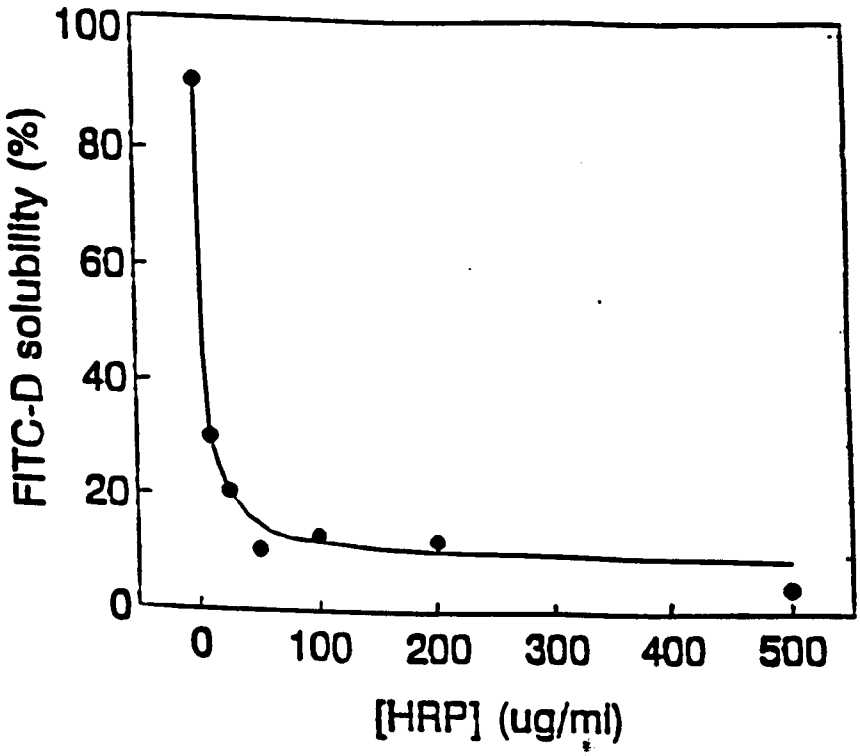

FIG. 1.2.1 FITC-D SOLUBILITY AS A FUNCTION OF HRP CONCENTRATION

Cells were incubated at 37°C for 5 min in the presence of FITC-D (3 mg/ml) together with HRP at the indicated concentrations. After cooling on ice and washing, the crosslinking procedure was carried out and cell concentration determined prior to solubilization in 1% Triton X-100. Insoluble material was removed by centrifugation and fluorescent intensity measured in the supernatant, as normalized to cell number. For each HRP concentration, additional samples were used to measure maximum solubility (H_2O_2 omitted) and background signal (no FITC-D). After subtracting background signal, fluorescent intensity was expressed as a percent of maximal solubility as indicated.

Almost maximal detergent insolubility of FITC-D (90%) was achieved by DAB-crosslinking in intact cells at HRP-concentrations above 50 μg/ml. A combination of FITC-D and HRP could, therefore, be used as a measure for the colocalization of these two fluid-phase markers in endocytic organelles. In the experiments to follow, HRP was used at a concentration of 200 μg/ml, unless stated otherwise.

1.3 THE EFFECT OF CELL NUMBER ON LIGHT SCATTERING DURING FLUORESCENT MEASUREMENTS

Due to limits in number of cells in each sample and feasible FITC-D concentration (3mg/ml), only a weak fluorescence signal was obtained. The optimal emission wavelength was determined, which would ensure maximal resolution of the fluorescence signal from the light scattering peak, cf. FIG. 1.3.1

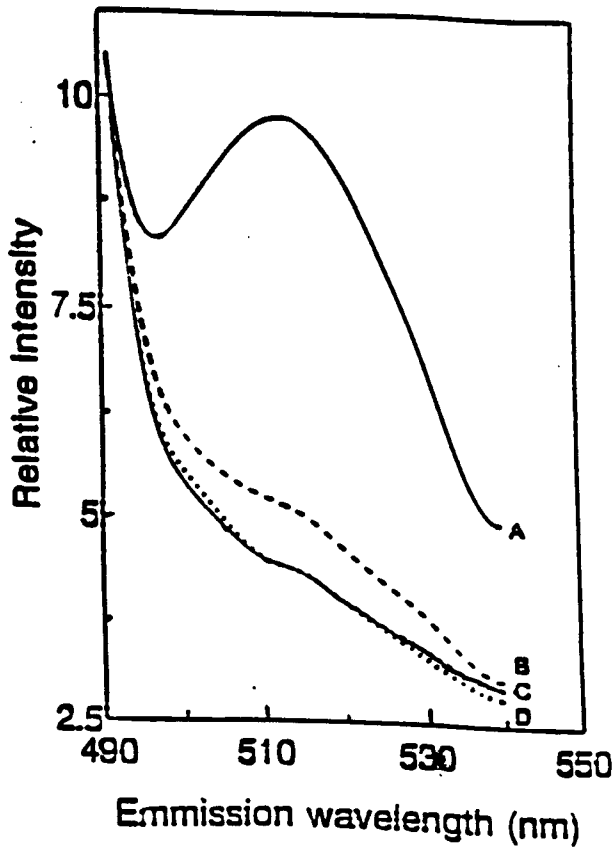

FIG 1.3.1 EMISSION SPECTRA FOR THE DETECTION OF FITC-D FROM SOLUBILISED CELLS IN RELATION TO DAB-CROSSLINKING

Cells were incubated at 37°C in the presence of FITC-D and/or HRP for 5 min. The crosslinking procedure was carried out and cell concentration determined prior to solubilisation in 1% Triton X-100. Insoluble material was removed by centrifugation and emission spectra of fluorescence intensity measured in the supernatant. The samples were scanned at a fixed excitation wavelength of 470 nm and the emission wavelength was varied in increments of 5 nm. The fluorescent intensity was normalized to cell number and the data were linked by cubic spline curve fitting.

The four curves in FIG. 1.3.1 represent the following samples, **A**: maximal fluorescence after the DAB-reaction in the absence of exogenous HRP, **B**: minimal fluorescence remaining after maximal trapping of FITC-D by DAB-crosslinking in the presence of HRP, **C**: background spectrum in the absence of FITC-D, after DAB-crosslinking in the absence of HRP and **D**: same as C, but in the presence of HRP. Minimal solubility was calculated from the intensities at 515 nm as (B-D)/(A-D) = 12%.

In a non-crosslinked sample (curve A), the fluorescent peak was clearly resolved from the dominating light scattering peak (on the left side of the fluorescence peak). Maximal fluorescence occurred at an emission wavelength of 515 nm. Accordingly fluorescence measurements in subsequent experiments were done at an emission wavelength of 515 nm. In the case of maximal trapping of FITC-D by DAB-crosslinking (curve B), only a slightly increased signal above light scattering (curves C, D) was observed. Light scattering contributed about one third to the maximal fluorescent intensity. Therefore, it was important to correctly account for this background signal.

In order to determine the extent to which soluble FITC-D and background signal varied with cell concentration in the sample, an experiment as in FIG. 1.3.2 was done.

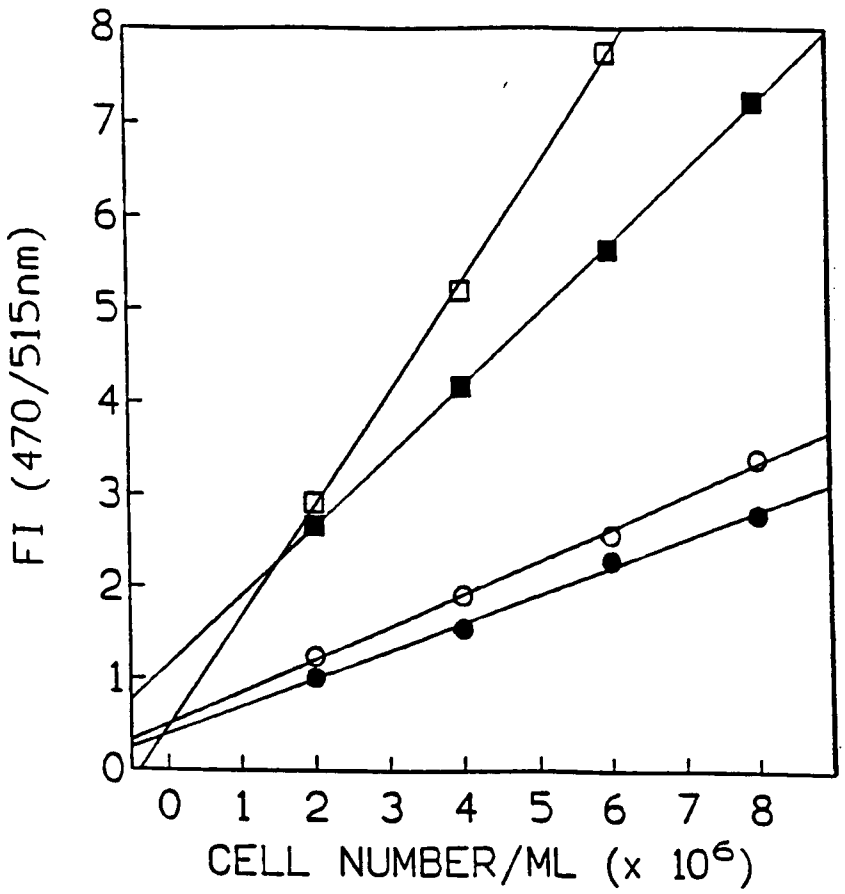

FIG. 1.3.2 EFFECT ON BACKGROUND FOR VARYING CELL CONCENTRATIONS IN RELATION TO FLUORESCENCE INTENSITY

Two samples (S and C), each containing an equal number of cells in RPMI-Hepes medium, were incubated at 37°C in the presence (S) or absence (C) of FITC-D and HRP (cells incubated in the presence of FITC-D for 5 min, cells then washed to remove excess FITC-D follwed by a 15 min incubation with HRP). Sample C, was to be used for background measurements, i.e. absence of ligand. The cells from both samples were washed separately and were then equally divided further, giving samples S^- (□), S^+ (■), C^- (o) and C^+ (●). DAB was added to all four samples but only one of each pair (S^+ and C^+) was crosslinked (addition of H_2O_2). Solubilization in 1% Triton X-100 was carried out and insoluble material removed by centrifugation. Sample S^- represented maximal FITC-D solubility and sample C^-, the uncrosslinked background sample. Each of the four samples were then divided to generate samples of increasing cell concentration as indicated.

In FIG. 1.3.2, fluorescent intensity increases linearly with cell concentration. Samples of maximal solubility (□ and ○) gave higher fluorescent values than their crosslinked counterparts (■ and ●). Background samples (○ and ●) were similar for all cell concentrations. However, the samples containing ligand (□ and ■) increasingly separated from one another as cell concentration increased.

Due to the fact that a restricted number of cells were available for each experiment, only one set of background samples (i.e. ○, ●) and duplicate maximum solubility samples (average value for 2(□) samples) were used as representatives for an individual experiment. Therefore, a variation in cell number between samples within an experiment were kept to a minimum.

In order to express the percent soluble FITC-D in a particular sample, the following calculation was used:

$$\text{Percent soluble FITC-D} = (■ - ●)/(□ - ○) \times 100$$

A minimal solubility value calculated in FIG. 1.3.1 at 515 nm was 12%. However, a value of 70% was calculated in FIG. 1.3.2 (for the data points at 4×10^6 cells/ml, for example). This discrepency is attributed to the different chase periods employed. In FIG. 1.3.1, FITC-D and HRP were simultaneously endocytosed whereas in FIG. 1.3.2, FITC-D

uptake was followed by a 10 min chase period prior to the addition of HRP to the medium. This delayed uptake of HRP was responsible for the higher FITC-D solubility value.

CHAPTER 2

EARLY ENDOSOME PROCESSING

2.1 INTERMINGLING OF FLUID-PHASE MARKERS IN EARLY ENDOSOMES

Previous studies have shown that a few minutes after uptake, endocytic contents no longer intermingles with subsequently endocytosed marker (Ajioka and Kaplan, 1986; Salzman and Maxfield, 1988 and 1989; Ward *et al.*, 1990 and Dunn and Maxfield, 1992). In contrast, Stoorvogel *et al.* (1991) have claimed that endosomes remain fusogenic during the entire prelysosomal endocytic pathway. Temporal segregation of endocytic contents is difficult to explain in terms of vesicular traffic model. However, in the special case where endosomal maturation involves the decline in fusogenicity of early endosomes to become non-fusogenic endosomes, temporal segregation of endocytosed markers will result. The experiment described in FIG. 2.1.1 was undertaken to establish whether temporal segregation of endocytosed marker occurred in $P388D_1$ macrophage cells, and if so, to determine the kinetics of this process.

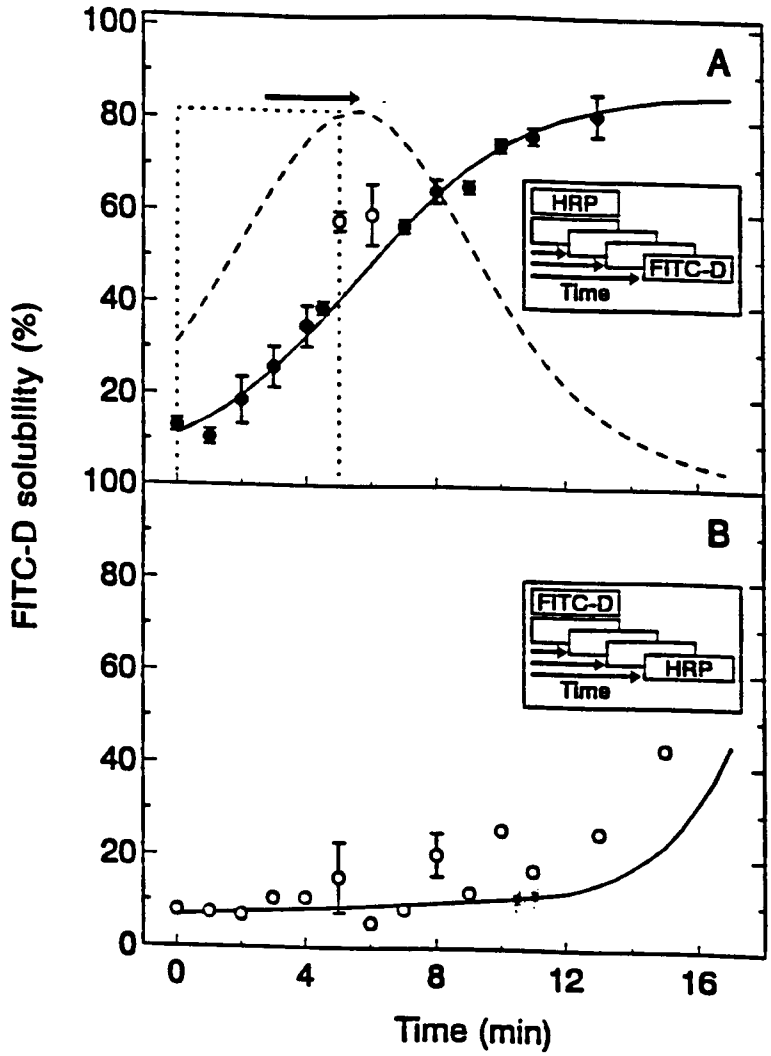

FIG. 2.1.1 INTERMINGLING OF FLUID-PHASE MARKERS IN EARLY ENDOSOMES.

(A) Cells were incubated in the presence of FITC-D for 5 min at 37°C. HRP (1 mg/ml) was added for 5 min, either simultaneously (at t = 0 min), or as increasingly delayed steps of 1 min. Eg., for the time point of 3 min, HRP was added after 3 min, i.e. during the last 2 min of FITC-D uptake. Then exogenous FITC-D and HRP were washed from the cells on ice, followed by further 3 min incubation at 37°C in the presence of HRP alone to complete the 5 min pulse of HRP uptake. Cells were cooled, washed, subjected to DAB-crosslinking procedure, counted, and solubilised in 1% Triton X-100. Insoluble material was removed by centrifugation. Fluorescence intensity in the supernatant was measured,

normalized to cell concentration and related to the fluorescence intensity from control samples where the DAB-reaction was mimicked in the absence of H_2O_2. The symbols represent the average value from three independent experiments. Higher solubility levels for samples of times 5 and 6 min (O) could be ascribed to a delayed first uptake of HRP after the washing step on ice for the removal of FITC-D and were not considered for evaluation. The solid line was fitted as a sigmoid curve (Graphpad: Inplot version 4.03) and indicated the time course for appearance of endosomes in the non-fusogenic state. Upon differentiation of the sigmoidal curve, the position of maximal accumulation rate was observed at approximately 5.5 min. With the center of the administered pulse of FITC-D at 2.5 min, a maturation time of about 3 min was indicated (cf. arrow).

(B) The results of the inverse application of the fluid-phase markers, as indicated by the inset, are represented by the data points (O). These results could also be predicted by calculating the fraction of fusogenic endosomes at the various time points in (A) as a percentage of the maximum FITC-D solubility value. The values were plotted (not shown) and the solid line drawn from point to point (see following text for further details).

The solid curve, in FIG. 2.1.1 (A), depicting sigmoidal kinetics, shows an increase in FITC-D solubility as FITC-D-containing organelles pass beyond the 5 min "time window" (as defined by the 5 min HRP uptake pulse, dotted rectangular area). Upon differentiation of the sigmoidal curve, a bell-shaped "age" distribution profile resulted. The decrease in intermingling, implies a decline in fusogenicity of FITC-D containing endosomes with HRP in organelles of the 5 min time window. This decline was fastest at a time of about 5.5 min, corresponding to the steepest part of the slope on the sigmoid curve. In relation to the center of the 5 min uptake pulse of FITC-D (dotted rectangle), this distribution was displaced by about 3 min,

and thus representing an average time for the maturation process to occur. After maturation, endosomes were no longer intermingling their contents (fluid-phase marker) with that of newly formed endosomes.

The two fluid-phase markers, HRP and FITC-D, are not simply interchangeable in this experimental approach. The reason for this is the non-linear dose-response curve (FIG. 1.2.1) which formed the basis for the detection of HRP: A small amount of HRP being delivered into FITC-D-containing endosomes could suffice to render all FITC-D insoluble; In contrast, a small amount of FITC-D being delivered into HRP-containing endosomes would only be detected as an accordingly small fraction of FITC-D becoming insoluble.

This difference between the two markers could be exploited to obtain further proof for the change in fusogenicity during the maturation process by inverting the uptake pulses of the two markers (FIG. 2.1.1 (B)). From the sigmoid curve in FIG. 2.1.1 (A) the fraction of (now HRP-containing) endosomes which remained fusogenic at a particular time (say 10 min) was determined, eg. 16% at 10 min. Because of their fusogenicity, these endosomes would intermingle their contents (HRP) with the entire fusogenic endosome population (constant due to homeostasis) which contained newly entered FITC-D (5 min time window). This would lead to a corresponding dilution of their HRP content (down to 16%). With a loading concentration of 1000 µg/ml, HRP would, therefore, still be present at 160 µg/ml. At this concentration, an FITC-D solubility of only 10.8% was predicted from the curve in FIG. 1.2.1. A curve calculated on the basis of these rather simple considerations (FIG. 2.1.1 (B)) corresponded closely to the experimental observations.

The above scenario, based on HRP dilution due to intermingling, would predict substantially different results for lower loading concentrations of HRP which are closer to the critical concentration required for efficient crosslinking (> 50 µg/ml, cf. FIG. 1.2.1).

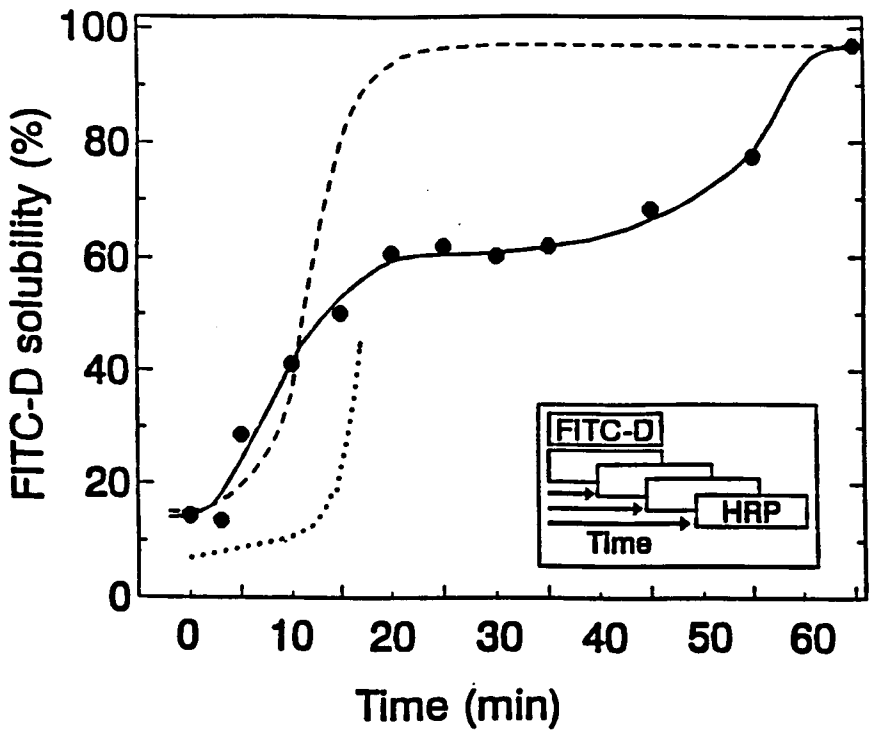

FIG. 2.1.2 INTERMINGLING IN EARLY ENDOSOMES USING A REDUCED HRP CONCENTRATION (50 μg/ml)

The protocol followed in this experiment was the same for FIG. 2.1.1 (B), excepting for the HRP concentration (50 μg/ml vs. 1 mg/ml). The averages from duplicate values are shown from a single experiment. The solid line curve was drawn by eye. The experimental outcome was predicted as shown by the dashed line, calculated as explained in the text related to FIG. 2.1.1. Good agreement with experimental observation was obtained for $t < 10$ min, when compared to the substantially different prediction as for the case in FIG. 2.1.1 (B) (solid line, shown in FIG. 2.1.2 as a dotted line).

The results in FIG. 2.1.2, using 50 μg HRP/ml, show a correspondence between prediction and experimental outcome for only the lower half of the sigmoidal curve (cf. data points and dashed line for $t < 10$ min).

For t > 10 min, FITC-D solubility started to diverge from the predicted values, reaching an intermediate plateau of 60% for times between 20 and 35 min, before full solubility was observed for t ≥ 60 min as a result of full HRP depletion. The level of 60% solubility corresponded to an intraendosomal HRP concentration of about 3 μg/ml (cf. FIG. 1.2.1). Observing this plateau was unexpected. One explanation could be that small amounts of HRP are returned to the fusogenic endosomes via fusion with recycling vesicles.

2.2 INTERMINGLING OF MARKERS IN EARLY ENDOSOMES AT 27°C

Original experiments to study segregation of constituents along the endocytic pathway were done with Tf-HRP (HRP conjugated to transferrin) as a marker (Ajioka and Kaplan, 1986). Because of the rapid cycling time of this receptor, experiments were done at lower temperatures in order to obtain a better resolution in time. We therefore, repeated the experiment, whose results are presented in FIG. 2.1.1 (A), at 27°C to establish correspondence with this earlier work. Due to an approximately 4-fold lower endocytic uptake rate of FITC-D (and HRP) at 27°C, the pulse times were doubled from 5 to 10 min to obtain a sufficiently strong signal of fluorescence measurement. The result is shown in FIG. 2.2.1. The maturation time at 27°C was 8 min which

turned out to be about twice as long than at 37°C (cf. 3 min, as in FIG. 2.1.1).

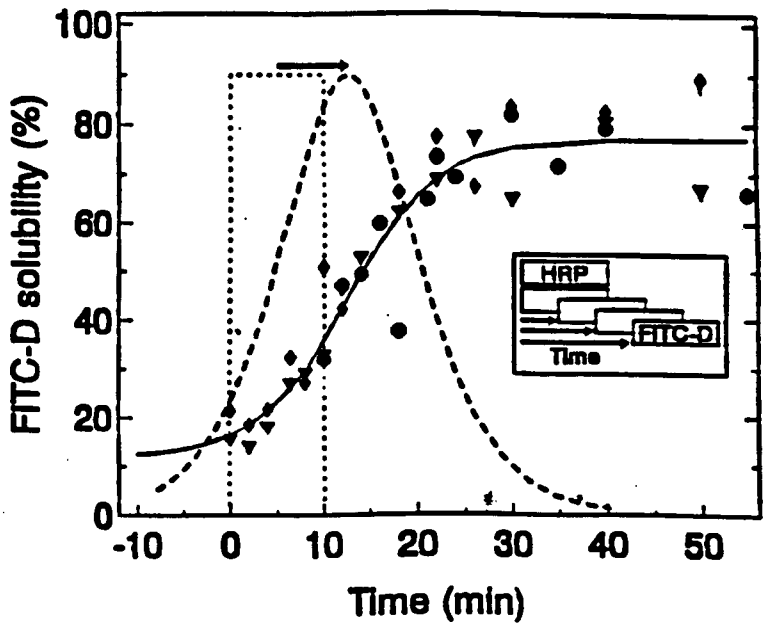

FIG. 2.2.1 INTERMINGLING OF FLUID-PHASE MARKERS IN EARLY ENDOSOMES AT 27°C

The protocol followed was as given in FIG. 2.1.1, except that a longer incubation period for the fluid-phase markers was used. The different symbols (▼,●,♦) refer to average values from duplicate samples in three independent experiments. A sigmoid curve (solid line) was fitted to the data (Graphpad: Inplot version 4.03) and upon differentiation (dashed line) indicated an endosome maturation time of about 8 min (arrow).

CHAPTER 3

LYSOSOMES: THE 'END POINT' OF THE ENDOCYTIC PATHWAY

In the previous chapter we gave evidence that the maturation model adequately describes the early stages of the endocytic pathway. The question can now be asked whether maturation accounts for delivery of endocytic contents to lysosomes. Storrie et al. (1984); Roederer et al. (1987 and 1990) and Stoorvogel et al. (1991) support the notion that the appearance of endocytic material within dense lysosomes reflects a maturation event rather than a process requiring fusion of endocytic vesicles with preexisting dense compartments.

Lysosomes are the major sites of accumulation and degradation of internalized macromolecules. Accordingly, lysosomes are expected to be an endocytic compartment where final intermingling of endocytic contents may occur.
In this chapter the kinetics of the delivery of endocytic markers to lysosomes will be considered. Processing and transport of early endosomal contents to the lysosomes can either occur by vesicular traffic or by maturation. However, since lysosomes are themselves known to fuse with one another (Ferris *et al.*, 1987), either model may eventually lead to intermingling of contents. To distinguish the two

models from one another, both the kinetic and quantitative aspects related to intermingling were investigated. An almost immediate appearance of contents marker at all stages of the endocytic is indicative of a first-order kinetic process and a maturation process will lead to the progressive processing of marker from one compartment to another following each respective maturation period, represented by a zero-order process.

3.1 DELIVERY TO LYSOSOMES

Direct observation of appearance of endocytosed marker in lysosomes was achieved by isolating the endosomes from the lysosomes, based on differences in their densities on a percoll gradient. Therefore, quantitative amounts of marker could be determined for both fractions. As indicated by the curve in FIG. 3.1.1, endocytic marker accumulated in lysosomes by first-order kinetics with $T_{\frac{1}{2}}$ = 5.5 min.

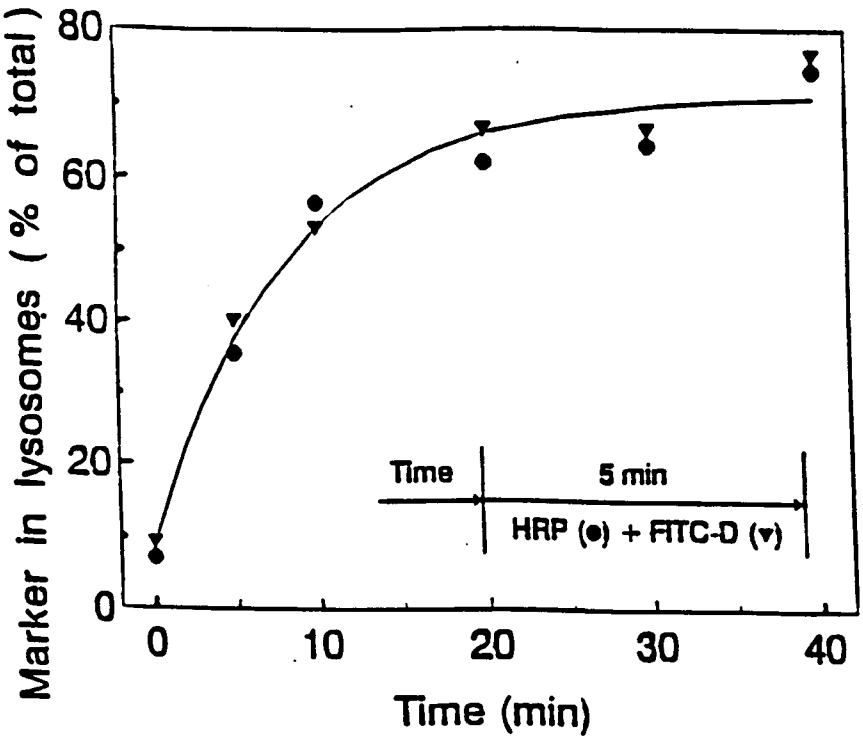

FIG. 3.1.1 ACCUMULATION OF FLUID-PHASE MARKERS IN HIGH-DENSITY LYSOSOMES

Cells were incubated in the presence of HRP and FITC-D for 5 min. Markers were removed by washing on ice. Cells were reincubated at 37°C in the absence of fluid-phase markers for the indicated times, cooled on ice and subjected to cell fractionation to determine the fraction of marker in high-density lysosomes on Percoll density-gradients. Recovery of lysosomes in high-density fractions was measured via the lysosomal enzyme, ß-N-acetylaminodeoxyglucosidase (NAGAase) (cf. (vii) Materials and Methods). Amounts of marker were normalized to 100% recovery and were expressed as a fraction of the total amount of marker in each gradient. Data points (●,▼) were obtained as average values from duplicate gradients during a single experiment and the line was drawn using Graphpad: Inplot version 4.03.

The exponential curve in FIG. 3.1.1 is not indicative of a maturation process as accumulation of product at the lysosomal level can not occur by first order kinetics. For a maturation process, the curve would have been sigmoidal in shape. The data therefore suggest that a vesicular traffic process was involved in the delivery of endocytic contents from the late endosomes to lysosomes. The apparent immediate appearance of ligand at the lysosomes is due the samples having been taken following an initial 5 min uptake of ligand by the cell (see inset).

It could be expected that sequentially endocytosed fluid-phase markers might become intermingled in high density lysosomes. This was tested by chasing successive pulses of FITC-D and HRP towards later stages of the endocytic pathway. The results are shown on the following two pages (FIG. 3.1.2).

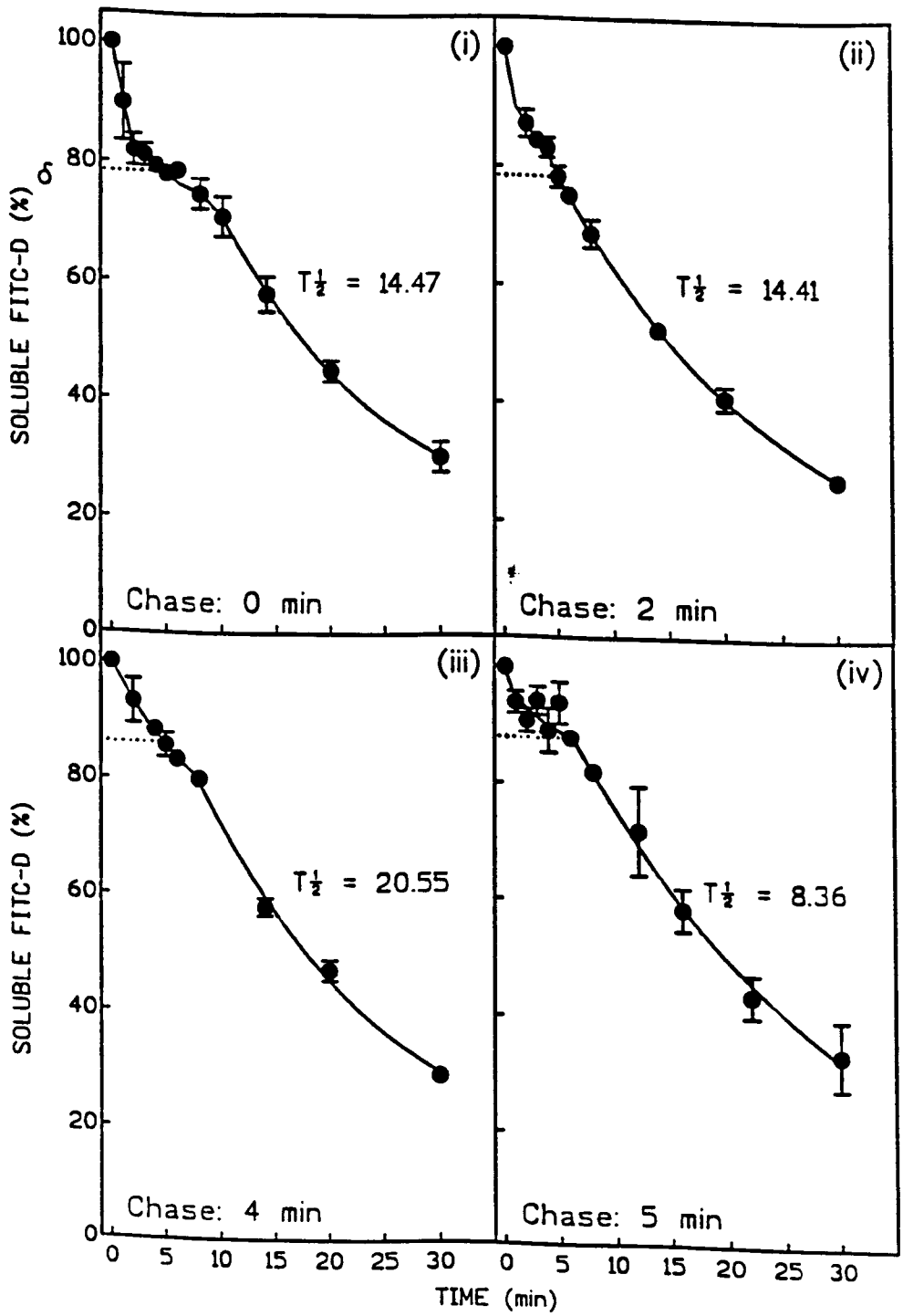
(i)
(ii)
(iii)
(iv)
T½ = 14.47
T½ = 14.41
T½ = 20.55
T½ = 8.36
Chase: 0 min
Chase: 2 min
Chase: 4 min
Chase: 5 min
SOLUBLE FITC-D (%)
TIME (min)
0
20
40
60
80
100
0
5
10
15
20
25
30

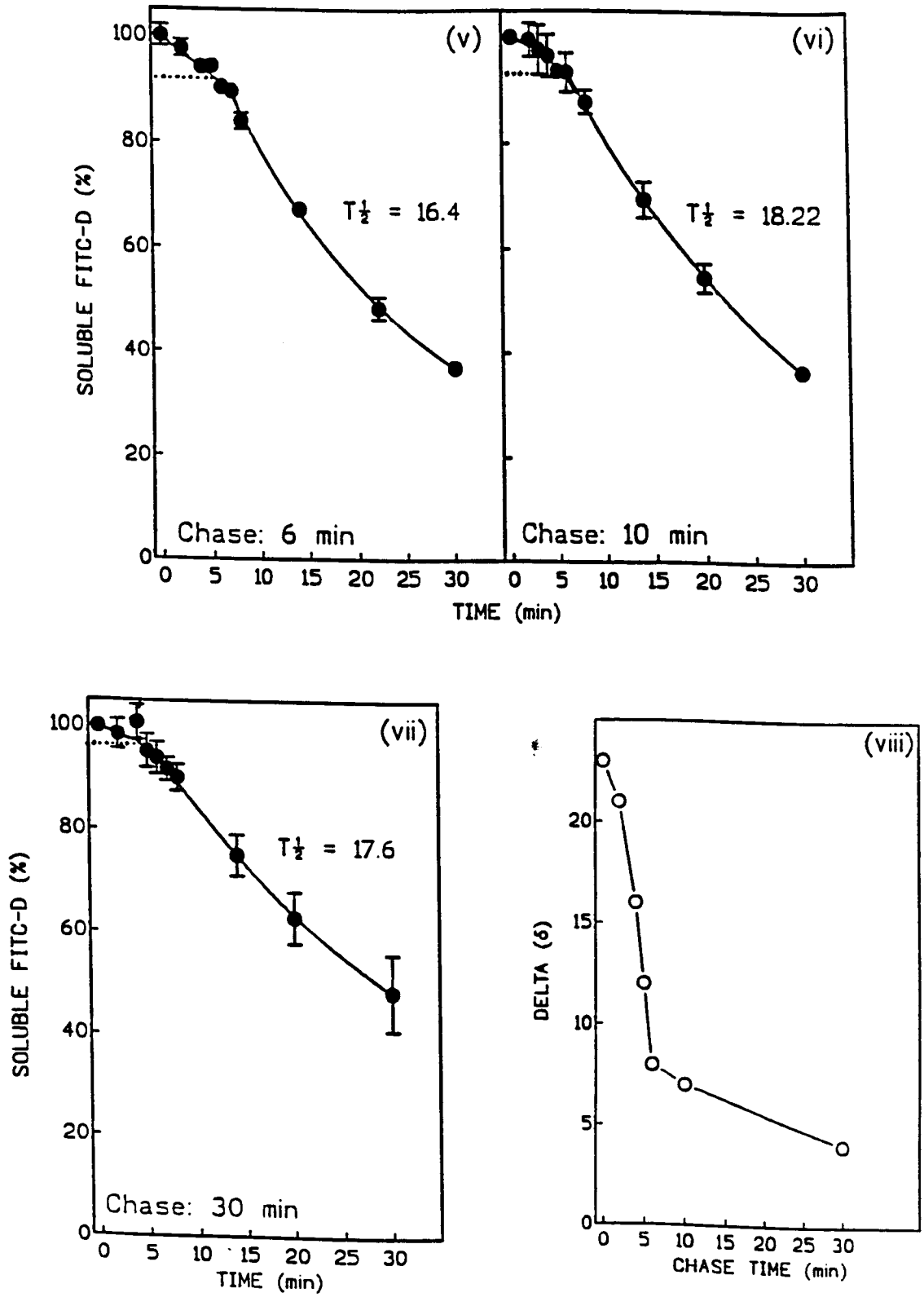

FIG. 3.1.2 INTERMINGLING IN LATER STAGES OF THE ENDOCYTIC PATHWAY

In FIG. 3.1.2, cells were incubated in the presence of FITC-D for 5 min. After this marker was removed by washing on ice, the cells were reincubated in the presence of HRP, either immediately (chase 0 min, (i)), or after a chase period of either 2, 4, 5, 6, 10 and 30 min, (ii - vii respectively). At the indicated times after the addition of HRP, cells were cooled and treated for determining the solubility of FITC-D after DAB- crosslinking. Maximal solubilities (t = 0; about 90%) were normalized to 100% to allow comparison between independent experiments. Points represent an average of 3 samples within a single experiment. Using GraphPad: Inplot version 4.03 the exponential curves were fitted and the initial points (< 5 min) were joined from point-point. The dotted horizontal line on each graph (i - vii), intersect the profile at 5 min giving a percent soluble FITC-D value, this value subtracted from 100% represents the delta (δ) value. The δ value was then plotted against the chase time (see final graph). A rapid decline of intermingling for chase times < 6 min for the 5 min time points was observed.

When HRP uptake followed immediately after FITC-D (FIG. 3.1.2, (i)), a short initial phase (< 2 min) of rapid intermingling could be observed. This was due to a fraction (about 20%) of FITC-D still being in immature, fusogenic endosomes at the time when HRP uptake became effective in terms of DAB crosslinking. When the gap between FITC-D and HRP was increased, this initial phase of rapid intermingling became smaller since fewer FITC-D containing endosomes remained in the immature, fusogenic state when HRP was added. This decline (δ) in remaining early intermingling is shown in FIG. 3.1.2 (viii) as a function of chase time can be understood in terms of the later part of a sigmoidal curve as in FIG. 2.1.1. For a gap larger than 10 min intermingling in early endosomes was no longer observed.

The continued uptake of HRP, in all cases, led to an increasing degree of intermingling in later stages of the endocytic pathway (t > 5 min). The $T_{\frac{1}{2}} \approx 15$ min calculated represents the delivery rate of the late endosomes, containing endocytosed HRP, to reach the FITC-D-containing lysosomes. This was suggestive that delivery of endocytic marker occurred to a common preexisting compartment as would be the case for vesicular traffic.

3.2 INTERMINGLING AT THE LYSOSOMAL LEVEL

In order to determine the kinetics for lysosomal delivery on the basis of intermingling in lysosomes, the arrival of HRP in FITC-D-containing lysosomes was observed over a period of 60 min. The increased colocalization of HRP with FITC-D led to a decline in FITC-D solubility as indicated in FIG. 3.2.1.

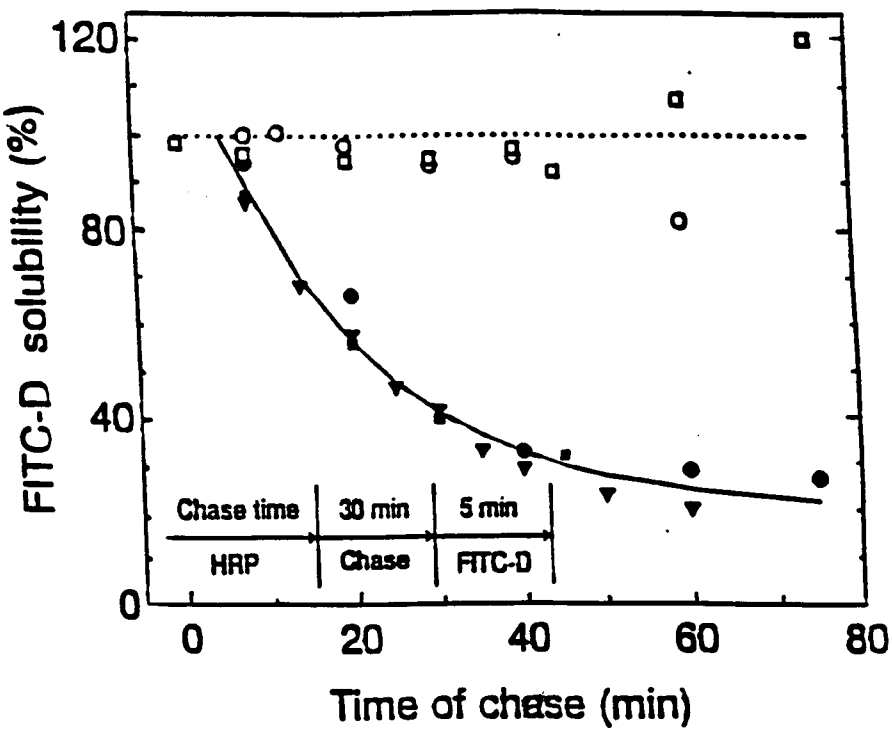

FIG. 3.2.1 INTERMINGLING OF HRP WITH FITC-D IN LYSOSOMES

Experiments were done exactly as in FIG. 3.1.2 (vii), where FITC-D was chased for 30 min prior to the addition of HRP. Data points were obtained from the average value of triplicate independent samples. The symbols (● , ▼) refer to independent experiments. Maximal values for solubility (91% on average), at t = 0 min, varied between experiments and were used for normalization to 100% solubility, as indicated. The best fit curve showed that colocalization, due to intermingling in lysosomes, increased by first-order kinetics with $T_{½}$ = 12 min. As a control for the intracellular stability of FITC-D, the experiment was simulated in the absence of HRP (□). As a control for inhibition of lysosomal delivery of HRP by Na^+-depletion (Ward *et al.*, 1990), a 60 min incubation in isotonic K^+ buffer was introduced after the 30 min chase period and prior to HRP uptake (○) (cf. Chapter 4).

The data in FIG. 3.2.1 showed that after a lag of about 5 min (as required for the maturation of newly formed HRP-containing endosomes, cf. above) colocalization of HRP with FITC-D in lysosomes increased by first-order kinetics, $T_{\frac{1}{2}}$ = 12 min. When lysosomal delivery of HRP was inhibited by Na^+-depletion, HRP did not intermingle with FITC-D in lysosomes (**O**), FIG. 3.2.1).

The half-life for intermingling in lysosomes, as observed in FIG. 3.2.1, ($T_{\frac{1}{2}}$ = 12 min) was significantly longer than for the appearance of HRP in lysosomes when measured directly by cell fractionation ($T_{\frac{1}{2}}$ = 5.5 min, FIG. 3.1.1). The reason for the increased half-life was due to an additional parameter, that of intermingling of the fluid-phase markers where HRP delivery to lysosomes was measured as a function of the FITC-D solubility. By changing the sequence of uptake for the two markers, FITC-D delivery can then be measured directly as a function of FITC-D solubility. The assumed rate-limiting step of intra-lysosomal spreading of HRP could be circumvented by preloading HRP into lysosomes and allowing time for proper diffusion. Such an experiment required simply to interchange the order in which the two fluid-phase markers were applied, the results are shown in FIG. 3.2.2.

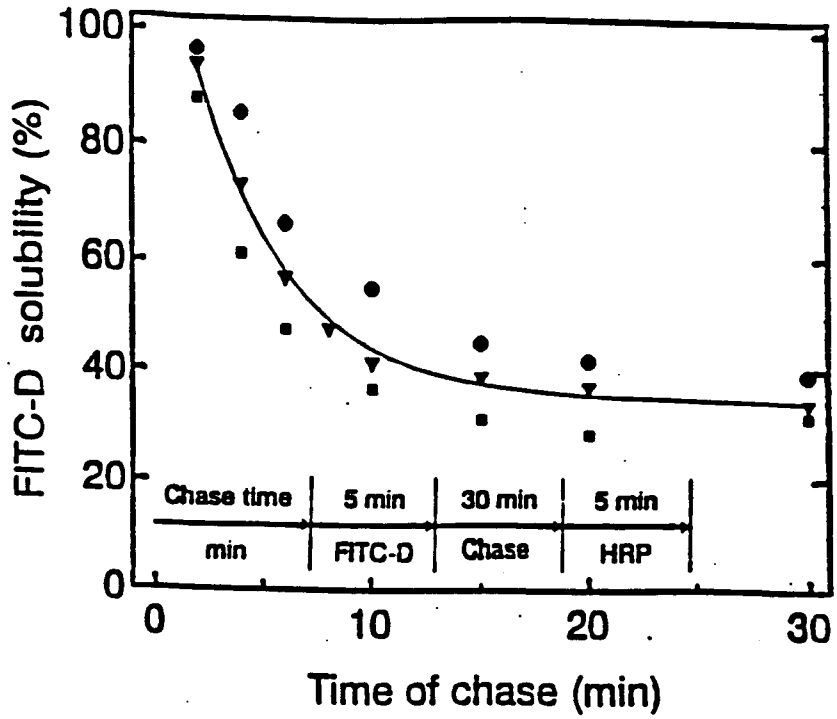

FIG. 3.2.2 INTERMINGLING OF FITC-D WITH HRP IN LYSOSOMES

Cells were incubated in the presence of HRP for 5 min. HRP was then removed by washing on ice, and cells were reincubated for 30 min (■ , ▼) or 60 min (●) to chase HRP into lysosomes. At the end of a the chase periods, FITC-D was added for 5 min. Cells were washed on ice to remove external FITC-D, reincubated for the indicated times, and FITC-D solubility determined after DAB crosslinking. Data points were the average of triplicate samples within a single experiment, with different symbols representing independent experiments. Error bars were similar as in FIG. 3.1.2. As indicated by the curve, FITC-D encountered HRP in lysosomes by first-order kinetics, $T_{1/2}$ = 3 min.

The exponential decay profile reflects an immediate decrease in the FITC-D solubility thus indicating that delivery occurred by first-order kinetics with $T_{1/2} \approx 4$ min, thus similar to the direct observation via cell

fractionation (FIG. 3.1.1). Mullock *et al.* (1989) found that in a cell-free system the contents of late endosomes are transferred to high-density lysosomes with kinetics which are compatible with a first-order process, $T_{1/2} \approx 5$ min.

After a chase of HRP for 30 and 60 min (FIG. 3.2.2), it can be expected that most lysosomes contain HRP. Accordingly, all newly matured FITC-D containing endosomes encounter HRP upon their first random fusion event with lysosomes. The data in FIG. 3.2.1 and 3.2.2 support random vesicular traffic as the model for delivery to lysosomes. In conclusion, the data are compatible with a model where lysosomal delivery depends on the random encounter and fusion events between preexisting secondary lysosomes and carrier vesicles which are the maturation products of early endosomes.

3.3 DELIVERY OF FLUID-PHASE MARKERS TO LYSOSOMES AT LOW TEMPERATURE (27/16°C)

There have been a number of studies regarding the effect of low temperature on endosome-lysosome fusion (Dunn *et al.*, 1980; Stoscheck and Carpenter, 1984; Hopkins and Trowbridge, 1983; Pesonen *et al.*, 1984 and Roederer *et al.* 1987 and 1990). The general consensus has been reached that delivery of endocytic contents to lysosomes was inhibited at temperatures below about 20°C.

Haylett and Thilo (1991) have shown that at 16°C endosome-lysosome fusion is not inhibited. Appearance of endocytic marker in high density lysosomes is found to commence after a lag period of about 6 h. Endosome-lysosome fusion is a late step in the endocytic pathway and a number of earlier events must be considered as perhaps being affected by low temperature. Once an endocytic contents marker has passed this rate-limiting phase, endosome-lysosome fusion can be observed to continue at low temperature (Haylett and Thilo, 1991).

Based on the knowledge that a low incubation temperature slows the rate of endocytic uptake, it was decided to repeat the experiment in FIG. 3.1.2 (ii) to have a 'closer look' at early endosome processing (first 5 min of chase period), the results are shown in FIG. 3.3.1. HRP uptake and delivery to lysosomes at 27°C was the critical issue in this experiment and independent of the incubation temperature for FITC-D uptake and chase period (at 37°C, 5 min is the standard time used to insure the presence of a ligand in the entire endosomal compartment).

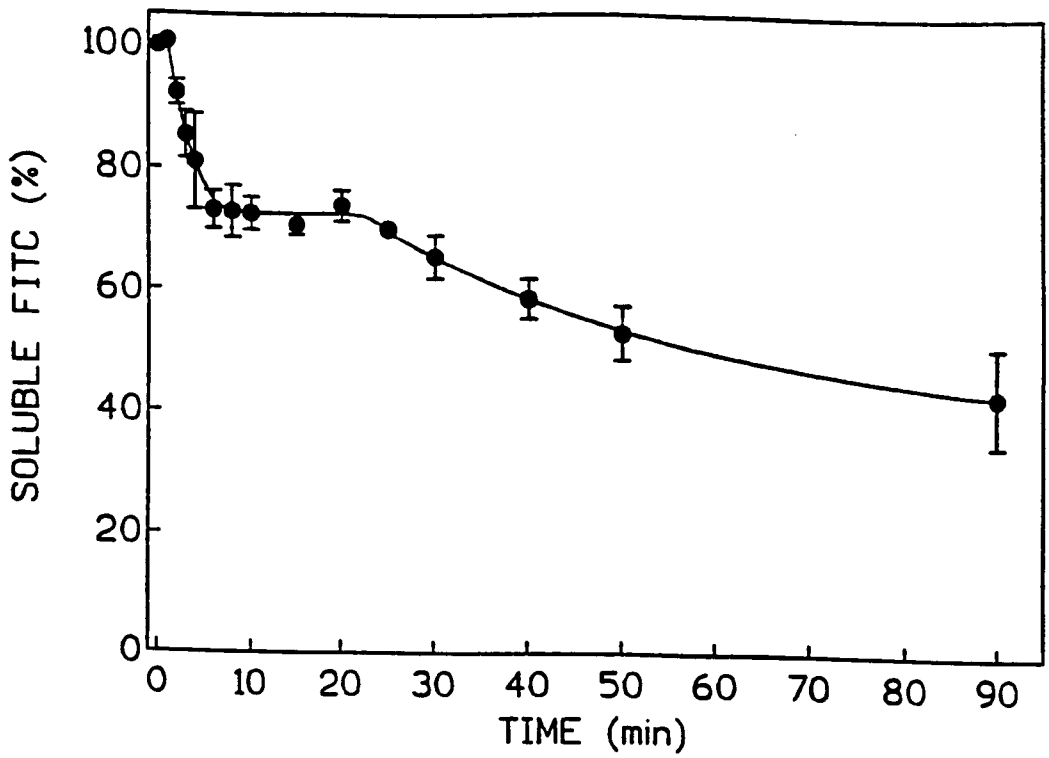

FIG. 3.3.1 DELIVERY OF FITC-D AND HRP TO LYSOSOMES AT 27°C

Early endosomes were loaded with FITC-D for 5 min (37°C), chased for 1 min (37°C), followed by HRP uptake for 90 min (27°C) during which samples were taken at the indicated time points (cf. legend FIG. 3.1.2). The data points represent average values from a single experiment. The exponential curve, starting at 25 min, was fitted by GraphPad: Inplot version 4.03 and the data points preceeding the exponential curve were joined from point to point. The $T_{\frac{1}{2}}$ for the curve was calculated to be 15 min.

The profile in FIG. 3.3.1 shows an increasing degree of colocalization of HRP with FITC-D. Initially an early phase ($t < 5$ min) of rapid intermingling of the markers was observed, followed by a plateau ($t = 5 - 25$ min) and finally a gradual decline in FITC-D solubility. The early phase of

intermingling represents HRP encountering the FITC-D still present in early endosomes. For t > 5 min, at 37°C, FITC-D has left the early endocytic compartment entirely, therefore the solubility of FITC-D remains unchanged. HRP then begins entering late endosomes and lysosomes and will start to intermingle with FITC-D once again leading to the further decline in FITC-D solubility (t = 25 - 90 min).

The effect on the delivery of HRP to lysosomes when decreasing the incubation temperature to 16°C is shown in FIG. 3.3.2. Due to the reduced rate of endocytosis at 16°C the incubation period with HRP was extended.

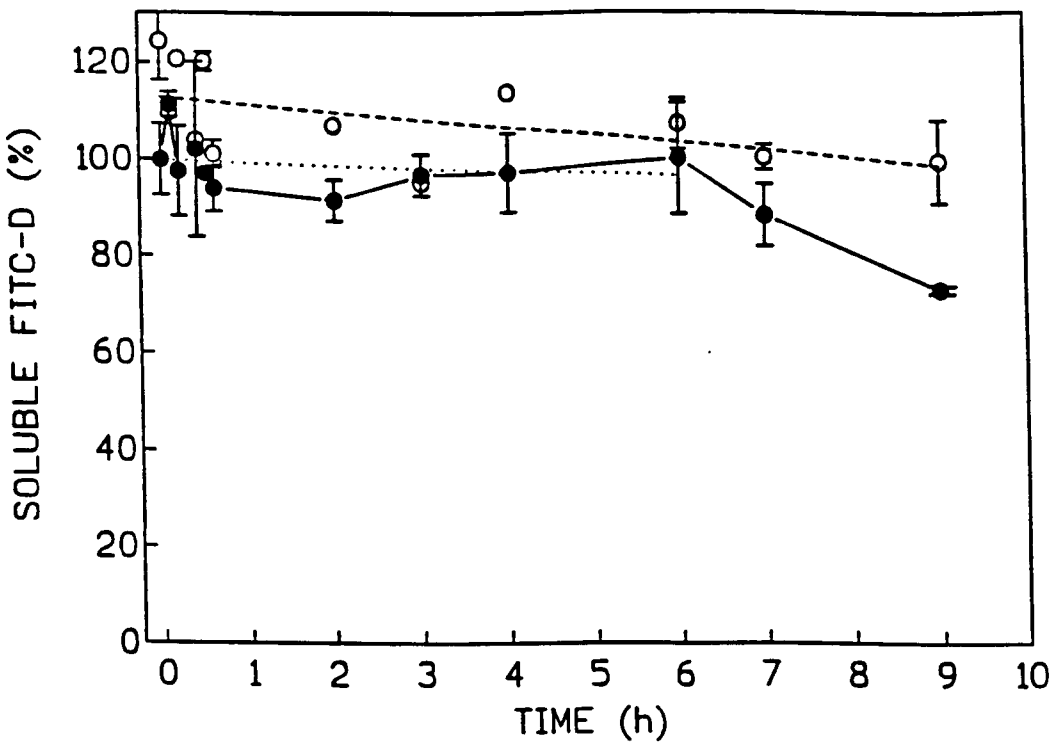

FIG. 3.3.2 DELIVERY OF HRP TO FITC-D CONTAINING LYSOSOMES AT 16°C

Cells were incubated in the presence of FITC-D for 5 min (37°C), followed by a 30 min chase period to deliver FITC-D to lysosomes. The cells were then incubated at 16°C for HRP uptake and samples were taken at the indicated time points during the 9 h incubation period (●). The average was drawn (dotted line) using linear regression (GraphPad: Inplot version 4.03). As a control for the stability of FITC-D, uncrosslinked samples were taken as well (o).

The results of FIG. 3.3.2 show that at 16°C HRP started to intermingle with FITC-D after 6 h. This conforms to the 6 h lag at 16°C as observed when studing lysosomal delivery via cell fractionation (Haylett and Thilo, 1991).

CHAPTER 4

THE EFFECT OF Na^+ DEPLETION AND BREFELDIN A (BFA) ON THE ENDOCYTIC PATHWAY

4.1 EFFECT OF Na^+ DEPLETION UPON LYSOSOMAL DELIVERY

Hepatocytes incubated in iso-K^+ buffer were reported by Baenziger and Fiete (1982) to internalize asialoglycoproteins, but that delivery to lysosomes was inhibited. Similar results were later shown by Wolkoff *et al.* (1984) and Ward *et al.* (1990) for hepatocytes and macrophages, respectively. The effect of an iso-K^+ buffer is thought to be due to an acidification of the cytosol (Samuelson *et al.*, 1988) which alters endosomal movement (Davoust *et al.*, 1987).

A Na^+-depleted (iso-K^+) buffer was used in FIG. 3.2.1 as a control for the inhibition of lysosomal delivery where the delivery of HRP to FITC-D-containing lysosomes was investigated. There is, however, the possibility that HRP was not endocytosed in the presence of a Na^+-depleted buffer, therefore having no effect on the FITC-D solubility.

To further investigate the effect of a Na^+-depleted buffer on the internalization and delivery it was decided to invert the sequence of markers endocytosed, as previously done in

FIG. 3.2.1 and 3.2.2 for a Hepes buffer. Endocytosis of FITC-D in a Na^+-depleted buffer could then be confirmed when measuring the solubility of FITC-D. The results are shown in FIG. 4.1.1.

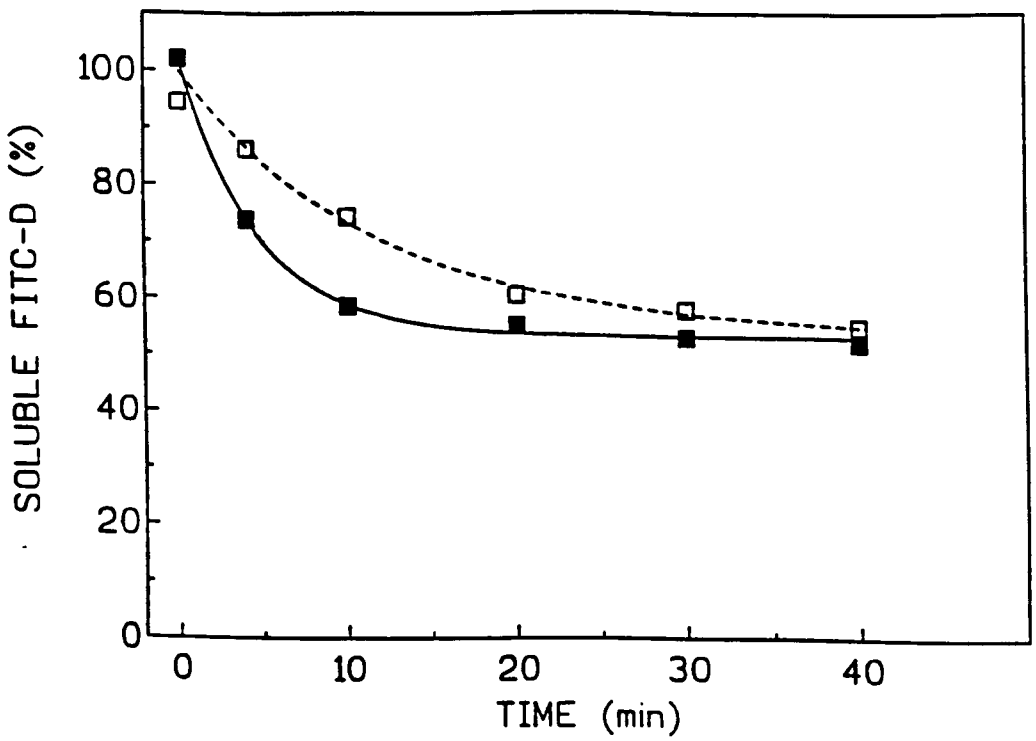

FIG. 4.1.1 INTERMINGLING OF FITC-D IN HRP-CONTAINING LYSOSOMES USING Na^+/K^+ AND K^+ BUFFERS

Cells were incubated at 37°C in a Na^+/K^+ buffer in the presence of HRP for 5 min, washed on ice and reincubated for 40 min to chase HRP to the lysosomes. The cells were resuspended either in a Na^+ buffer (Na^+/K^+) (□) or in a Na^+-depleted buffer (K^+) (■) and equilibrated in their buffers at 37°C for 60 min before FITC-D was added. After 5 min uptake, FITC-D was then chased to the lysosomes. At the indicated time points, samples were taken simultaneously for both buffers to measure the colocalization of the two markers. The data points represent the average value from two independent experiments and the curves were fitted by GraphPad: Inplot version 4.03.

The results in FIG. 4.1.1 show the colocalization of FITC-D and HRP in lysosomes for a Na^+/K^+ and K^+ buffer. The curve (dotted line) representing the situation for Na^+-depletion was unexpected. FITC-D was found to be internalized in the presence of a Na^+-depleted buffer and colocalization with HRP took place. If FITC-D had not been internalized, no fluorescence would then have been measured at all. The half-life for intermingling was 4 min when using a Na^+ buffer, which corresponds to FIG. 3.2.2 for FITC-D delivery to HRP-containing lysosomes, and 8 min for the Na^+-depleted buffer. Therefore, the Na^+-depleted buffer appears to reduce the rate of delivery of a fluid-phase marker to lysosomes. This contradicts the notion that Na^+ depletion inhibits lysosomal delivery (FIG. 3.2.1), however, there does appear to be a slight decline in the data points (cf. open symbols, FIG. 3.2.1) which implies that delivery to lysosomes was not totally inhibited. This decline could be attributed to a decrease in the HRP delivery to lysosomes in the presence of a Na^+-depleted buffer. A further interpretation could be that HRP may not be cleared entirely from the prelysosomal compartments thus causing a minimal effect on the FITC-D solubility.

4.2 EFFECT OF Na^+ DEPLETION ON DELIVERY TO, AND BUOYANT DENSITY OF, LYSOSOMES USING A PERCOLL GRADIENT

The following procedure was intended as a direct approach to examine the delivery of HRP to lysosomes in the presence of a Na^+-depleted buffer. RPMI-Hepes, Na^+ and K^+ buffers were used independently to compare their effects upon delivery. As before, lysosomes and endosomes were separated from one another by centrifugation on a 27% Percoll gradient (cf. FIG. 3.1.1). The density profile is represented in FIG. 4.2.1 to show that the 27% Percoll gradient ensured the complete separation of the endosomes and lysosomes from one another (previously undertaken by Haylett and Thilo, 1991).

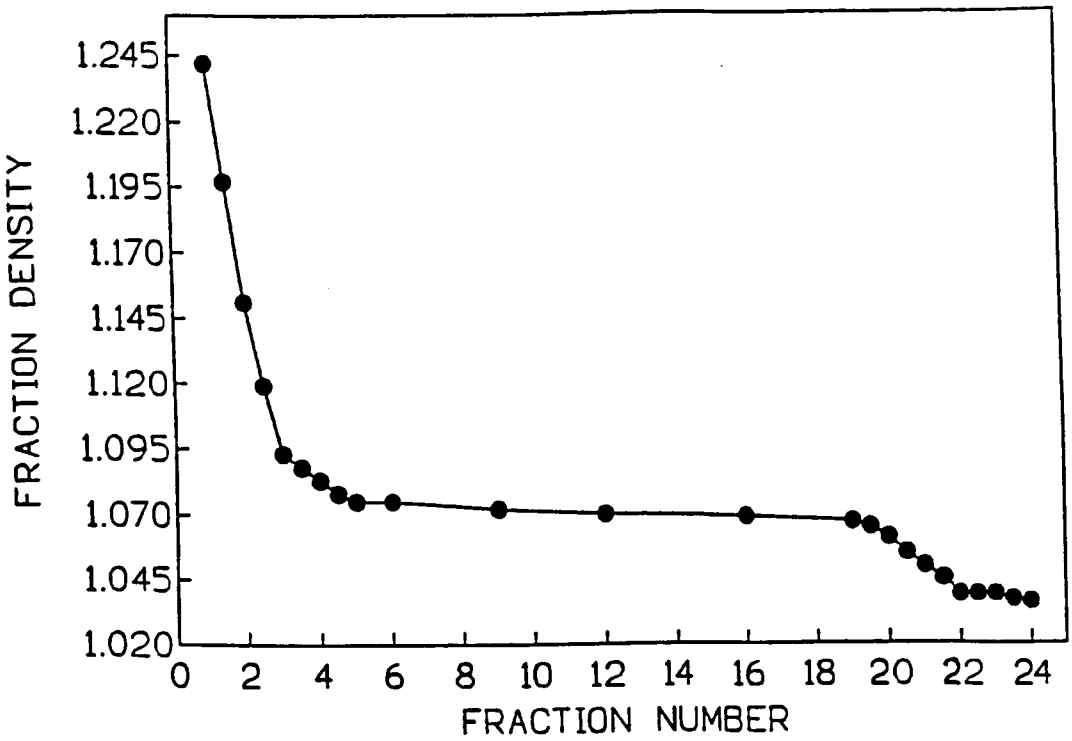

FIG. 4.2.1 DENSITY PROFILE OF A 27% PERCOLL GRADIENT

After centrifugation of the Percoll sample, (see Materials and Methods) fractions were taken and the density of each fraction was measured (D = M/V) and plotted against the fraction number of the sample (Haylett and Thilo, 1991).

The resulting density profile showed a clearly defined separation of the high and low density group fractions. This provided a highly efficient gradient which was required for the separation of high and low density components of the post-nuclear supernatant (PNS).

In order to be able to measure the amount of fluid-phase marker present in each fraction, the amount of NAGAase was first quantified to give a realistic estimation of the amount of ligand present in each fraction analyzed (see Materials and Methods). The intensity of NAGAase was measured for each fraction of the buffers and the data values plotted as shown in FIG. 4.2.2.

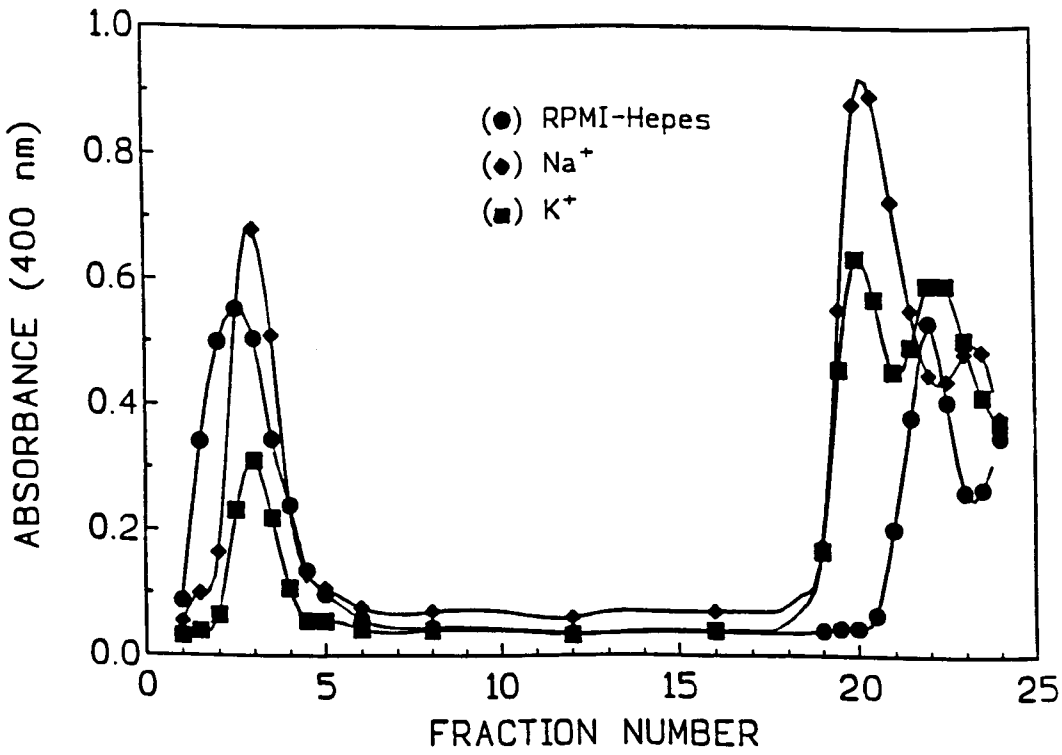

FIG. 4.2.2 NAGAase PROFILES USING VARIOUS BUFFERS

Cells were equilibrated in each buffer for 20 min, followed by a 5 min incubation period in the presence of HRP and chased for 40 min. The PNS was overlayed on a 27% Percoll gradient as described in Materials and Methods. The amount of NAGAase in each fraction was determined (see Materials and Methods for assay) and plotted against the fraction number. The three profiles represent the following buffers: (●) RPMI-Hepes; (♦) Na^+ and (■) K^+. Curves were fitted by cubic spline, GraphPad: Inplot version 4.03.

Fractions 1 - 6 represent the dense lysosomal fractions; 7 - 17, the background, 18 - 21, the endosomal fraction also containing light lysosomes, and 22 - 24 the soluble NAGAase due to vesicle breakage. NAGAase is clearly seen to be predominantly present in the high density/lysosomal fractions.

The delivery of HRP (similar results found for FITC-D, results not shown) to lysosomes could next be investigated using the same buffers as in FIG. 4.2.2. Cells were incubated in the presence of HRP for various periods of time (same protocol used as in FIG. 3.1.1). The profiles indicated in FIG. 4.2.3 below represent the 40 min incubation time period.

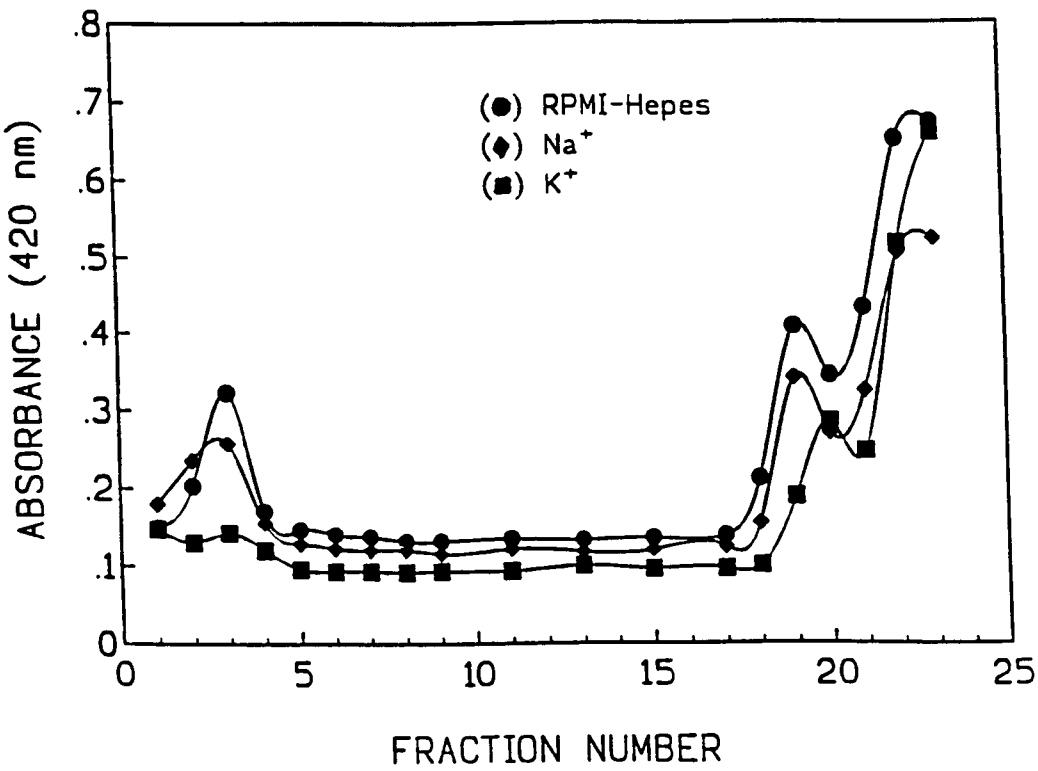

FIG. 4.2.3 HRP PROFILES USING VARIOUS BUFFERS

Incubations were carried according to the protocol described in FIG. 3.1.1. Following a 40 min uptake of HRP by the cells, an HRP assay (cf. (vi), Materials and Methods) was performed. The absorbance values of each fraction was plotted against the corresponding fraction number as represented by the data points. The symbols represent a particular buffer as indicated.

The amount of HRP delivered to lysosomes was calculated as the amount of lysosomal HRP ÷ Total HRP present (in both endosomes and lysosomes) X 100(%). The values for HRP were divided by their corresponding NAGAase value to obtain the relative amount of HRP delivered to lysosomes. The following results were obtained:

Lysosomes in RPMI-Hepes contained 31.46%;

Lysosomes in K^+ contained 24.52% and

Lysosomes in Na^+ contained 43.74%

HRP delivery to lysosomes (fractions 1 - 5) is not completely inhibited by the presence of a Na^+-depleted buffer, as indicated by the small peak on the profile (■). This reduced HRP delivery to lysosomes is supported by previous observations made regarding the delayed delivery of a ligand to the lysosomes in the presence of a Na^+-depleted buffer (FIG. 4.1.1).

To investigate the effect of a Na^+-depleted buffer on the lysosomal buoyant density, the NAGAase values (FIG. 4.2.2) for each buffer were plotted against the corresponding density values (FIG. 4.2.1). Having now both the density and the NAGAase values, a NAGAase-density profile can be constructed. The results are shown in FIG. 4.2.4.

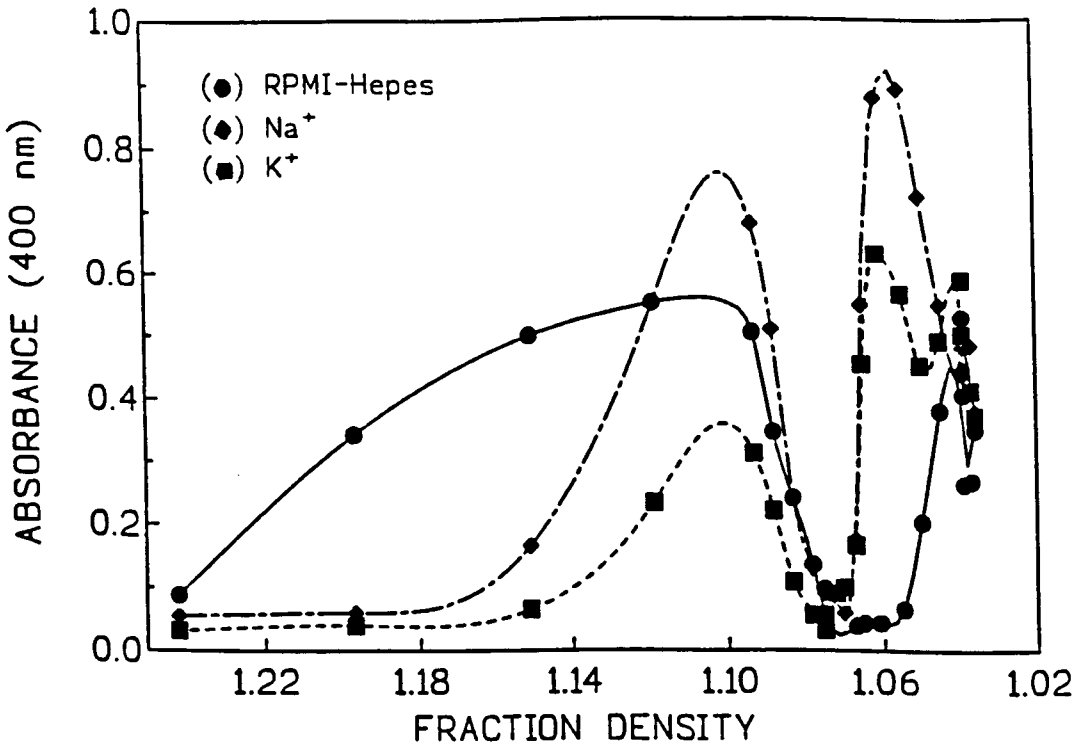

FIG. 4.2.4 NAGA-DENSITY PROFILES FOR THE THREE BUFFERS INVESTIGATED

The NAGAase values were plotted against the density gradient values for each corresponding fraction. The curves were fitted by cubic spline (GraphPad: Inplot version 4.03) and the different symbols represent a particular buffer as indicated.

The lysosomal profiles of the Na^+ and Na^+-depleted buffers showed a shift to the lower density region when compared to the lysosomal profile of the RPMI-Hepes curve, the Na^+-depleted curve (■) having the lowest overall density. Thus, a Na^+-depleted buffer may be said to cause a significant decrease in the lysosomal buoyant density.

These results contradict the previous assumptions that a Na^+-depleted buffer causes the inhibition of ligand delivery to the lysosomes. Instead, Na^+ depletion appears to cause a decrease in the lysosomal buoyant density and a decrease in the rate of delivery of an endocytosed marker to the lysosomes.

4.3 EFFECT OF BFA ON FLUID-PHASE UPTAKE ASSAYS

BFA has been shown to have profound effects on the morphology of various compartments of the endosome-lysosome system (Klausner *et al.*, 1992; Wood and Brown, 1992). The effects of BFA occur at low concentrations (10 μg/ml was used in this study), and are completely reversible (Pelham, 1991; Lippincott-Schwartz *et al.*, 1991). BFA causes membrane tubules derived from the trans-Golgi network (TGN) to fuse with early endosomes and plasma membrane (Hunziker *et al.*, 1992) producing an extensive tubulo-vesicular network that associates with microtubules while retaining early endosomal functions (Wood *et al.*, 1991). Results by Misumi *et al.* (1986); Lippincott-Schwartz *et al.* (1991) and Wood and Brown (1992) indicate morphological changes occurring within a cell, the most significant being the breakdown of the Golgi into numerous tubular processes (Lippincott-Schwatrz *et al.*, 1991). It remains unknown whether BFA affects transport from endosomes to lysosomes. Pelham (1991) pointed out that BFA has multiple species specific affects and that care should

be taken in interpreting the results on poorly characterized systems.

Preliminary experiments were undertaken to try and establish the effect of BFA upon the endocytic uptake by macrophages, the results are shown in FIG. 4.3.1.

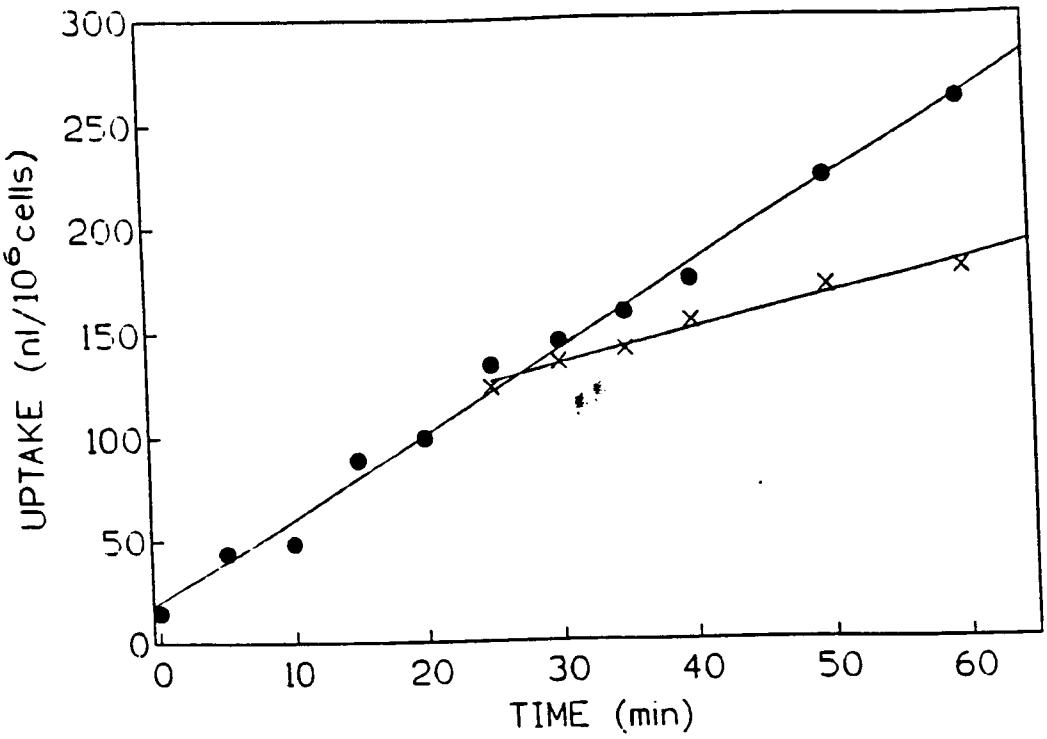

FIG. 4.3.1 FLUID-PHASE UPTAKE OF FITC-D AND THE EFFECT OF INTRODUCING BFA TO THE MEDIUM

A flask of cells in buffer were incubated at 37°C in the presence of FITC-D for 20 min while aliquots were taken at the indicated time points (●). The remaining buffer containing the cells was then placed on ice and these cells were pelleted and divided to give two samples containing equal number of cells. FITC-D was added to both samples, to allow the continued uptake of FITC-D, by the cells, and BFA added to only one of the flasks (x). Further aliquots were taken from both

samples at the indicated time points. The amount of FITC-D endocytosed was measured and calculated as $nl/10^6$ cells, these values were then plotted for their corresponding time points and linear regression was used to calculate the rates for each profile. The profile representing absence of BFA (●) had an endocytic rate of ≈ 3.8 $nl/10^6$ cells and the profile for presence of BFA (x) ≈ 1.2 $nl/10^6$ cells.

From the results in FIG. 4.3.1, it is clearly shown that as soon as BFA was added to the medium, at t = 20 min, an immediate effect on the endocytic uptake rate resulted as shown by the (x) data points, starting at 25 min.

The next question addressed was that which concerned the ability of cells to regain their 'normal' endocytic uptake rate following the elimination of BFA from the medium. The results of this experiment is shown in FIG. 4.3.2.

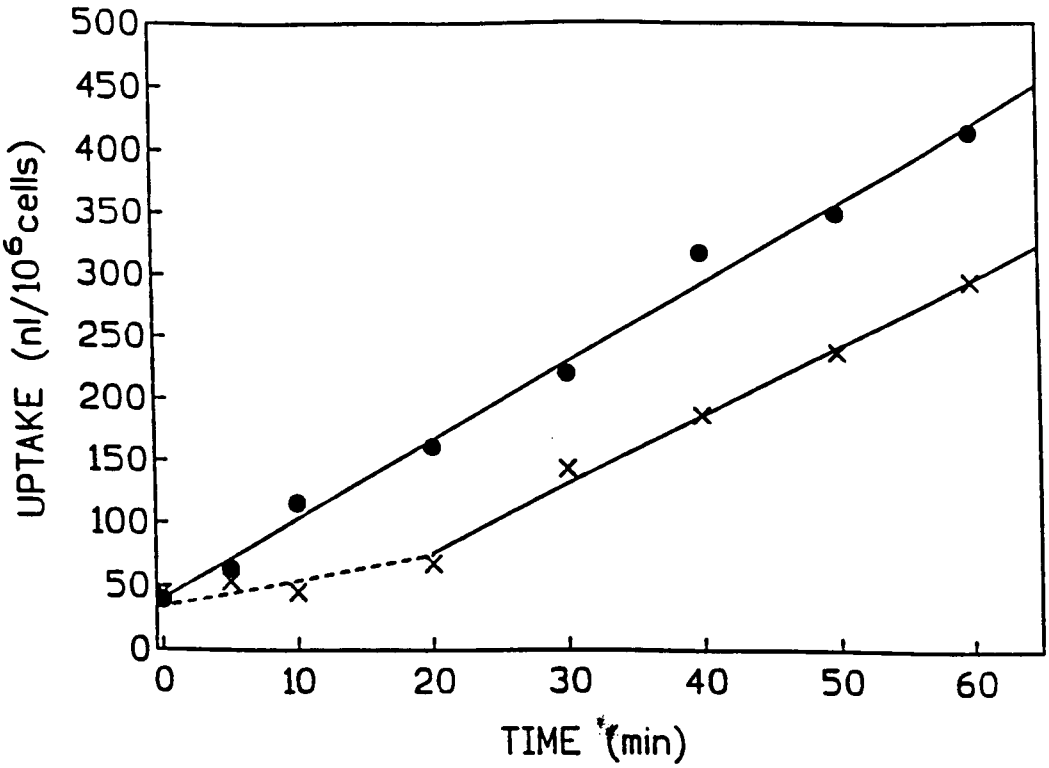

FIG. 4.3.2 RECOVERY IN THE ENDOCYTIC RATE FOLLOWING THE WITHDRAWAL OF BFA FROM THE MEDIUM

Two flasks (● and ✕), each containing an equal number of cells in buffer at 37°C, were incubated for 20 min in the presence of HRP and one flask additionally contained BFA (✕). During this 20 min incubation period (dashed line) aliquots were taken from both flasks at the indicated time points. The cells were then placed on ice, washed and resuspended, at 37°C, in the buffer containing HRP and samples were taken once again for a further 40 min. The cell number for each sample was determined and assayed for HRP uptake and plotted as a function of time. The linear regression profiles were drawn, indicated by the solid lines, (GraphPad: Inplot version 4.03) and the rates of uptake calculated: giving 6.0 nl/10^6 cells (●) and 4.25 nl/10^6 cells (✕).

The results show that the cells are capable of regaining a 'normal' fluid-phase endocytic uptake rate after the elimination of BFA from the medium (supported by Pelham (1991) and Lippincott-Schwartz *et al.* (1991)). In conclusion, it has been shown that BFA has a marked effect upon the endocytic uptake rate of macrophages, reducing the rate by almost four fold, BFA could therefore be used in further studies.

DISCUSSION AND CONCLUSION

Maturation of early endosomes

In this study the time course was determined by which labeled fusogenic endosomes, as a fraction of the entire and constant population of early endosomes, appear in a non-fusogenic state. On finding that this time course can be described by a sigmoid curve, it has been concluded that early endosomes become non-fusogenic by a process of maturation. Vesicular traffic between permanent early and late endosomes cannot account for the sigmoid decline in the intermingling of sequentially endocytosed markers.

The results in this study show that maturation of the early endosomes involves a decline of intermingling and accordingly of fusion. Early endosomes undergo a process of maturation to a state where they are no longer fusogenic towards early endosomes. The product of a maturation process (non-fusogenic endosomes) is not expected to accumulate by first-order kinetics. Such kinetics will occur only in the extreme case, where the maturation process is dominated by a single, rate-limiting, random step, in a series of faster random events which all form part of the maturation process.

The result in FIG. 2.1.1. shows that early endosome intermingling decreases with time, seen by the decline in the FITC-D-containing endosome fraction which remains

fusogenic towards early HRP-containing endosomes (in the 5 min time window). The reason for this decrease in intermingling is a result of the endosomes maturing to become late non-fusogenic endosomes. The average maturation time at 37°C was about 3 minutes (indicated by arrow in FIG. 2.1.1 (A)). The variation around this average value cannot be seen directly from the width of the bell-shaped curve in FIG. 2.1.1 (A). The observed half-width of about 9 minutes must be related to the 5 minute-width of the input pulse. The latter broadens to an extent which is related to the variation in maturation time within the population of maturing endosomes. This variation can be calculated to be ± 3.6 minutes (calculated in terms of a Gaussian distribution with σ = 3.6, calculation not shown; this is an approximation as required to make the calculation feasible although the actual data at $t < 2$ minutes are not symmetrical due to the constraints at $t = 0$). In view of the average maturation time of 3 minutes, this variation seems rather large. It probably reflects differences between different cells rather than within the endosome population of an individual cell.

Support for the above results is given as follows: Gruenberg and Howell (1987) found maximum fusion competence to occur in endosome fractions isolated 5 min after internalization; Salzman and Maxfield (1989) established that fusion continued for 5 to 10 min after the initial

internalization of the ligand into the cell and Ward *et al.* (1990) showed that newly formed endosomes lose their fusogenicity after 2 to 4 min (Fig. 2 in Ward *et al.*, 1990).

Dunn and Maxfield (1992) showed that, for CHO-cells after a pulse of endocytic uptake, individual endosomes retain their original endocytic load and that their number remains constant. The fraction of endosomes that intermingle their contents with subsequently endocytosed marker declines by apparent first order kinetics ($T_{\frac{1}{2}} \approx 3$ min, Fig. 5 in Dunn and Maxfield, 1992). This observation has been previously used to characterize the process of endosome maturation as a conversion from a fusogenic to a non-fusogenic state. As mentioned in this study, maturation is associated with a zero-order process. Dunn and Maxfield's (1992) observations should be seen rather as representing only the latter half of a sigmoidal curve as in FIG. 2.1.1 (A) (for the time > 5 min only, a $T_{\frac{1}{2}} = 3$ min could be mistakenly inferred, which would be in full agreement with their data. The data represented in FIG. 2.1.1 (A) for macrophage-like cells, therefore, are in quantitative (amplitude and time course) agreement with observations for CHO-cells.

The maturation model proposes the continuous *de novo* formation of early endosomes by numerous fusion events. Such a process should lead to extensive intermingling at the level of early endosomes, resulting in a constant new supply

of fusion-mediating constituents. Why then is there a loss in fusogenicity? An explanation could be that these constituents may be lost (possibly by membrane recycling) at a faster rate, thus causing individual endosomes to gradually loose their fusogenicity by first-order kinetics. These kinetics, however, have not been determined (*kinetics of maturation*). It is most important to realize the difference between the *kinetics of maturation* and *the kinetics by which matured product appears*. The later must follow sigmoidal kinetics, regardless of what the *kinetics of maturation* may be (as determined by the underlying mechanism, cf. above).

Support for the vesicular traffic model would require that a fluid-phase marker, once incorporated into early endosomes, would immediately start leaving towards late endosomes by randomly entering into budding vesicles (assuming rapid diffusional randomization within an organelle). Having arrived in late endosomes the marker would, for the same reason, proceed immediately towards the next stage and so forth. Therefore, the marker would appear in all stages of the pathway almost immediately after uptake. A second marker, once endocytosed, will equally start distributing itself to all consecutive compartments. Qualitatively, the two markers should be seen to colocalize entirely throughout the pathway.

Griffiths and Gruenberg (1991) argue in favour of the vesicular traffic model, proposing that early and late endosomes are permanent cell organelles. Support for the vesicular traffic model was also given by Merion and Sly (1983) based on their observations that internalized ligands were delivered to preexisting compartments in the endocytic pathway. However, the incubation of the cells in the presence of a fluid-phase marker exceeded 5 min (15 and 20 min respectively in both studies) and thus maturation of the early endosomes in the initial stages of the pathway of endocytosis was overseen and vesicular traffic assumed for the entire endocytic pathway. Therefore, the observed results can not be used in support of the vesicular traffic model for early stages of the endocytic pathway.

Lysosomal delivery by vesicular traffic

After establishing that maturation was involved during early endocytic processing, it was decided to investigate whether lysosomes are derived by the maturation of endosomes. Support for the maturation model is given by Storrie *et al.* (1984) where they reported that '*The rapid and progressive prelysosomal increase in pinosome density reported here suggests that a vesicle maturation process may be a normal step in the transfer of endocytic contents to lysosomes*'. Roederer *et al.* (1990) observed that isolated endosomes could undergo an increase in density *in vitro* in the absence of lysosomes, depending on ATP and

acidification, concluding that this mimics the density change which occurs *in vivo*.

Based on the observation that endocytic contents-marker is delivered to lysosomes by first-order kinetics (FIG's 3.1.1 - 3.2.2), it can be concluded that secondary lysosomes do not derive from a precursor organelle by a process of maturation. As mentioned above, first-order kinetics are incompatible with a maturation process. This led to the proposal that lysosomal delivery, indicated by the exponential curves, occurred by the random encounter and fusion events of the carrier vesicle, which are the maturation products of early endosomes, with the pre-existing secondary lysosomes.

Previous evidence that lysosomes are not derived by maturation has been reported for bone-marrow macrophages where macropinosomes, as identified in terms of fluid-phase contents marker, appear with a gradually changing membrane composition (maturation) before merging with a prelabeled, stable lysosome compartment (vesicular traffic) after about 9 minutes (Racoosin and Swanson, 1993). Further support for the vesicular model has also been given by Mullock et al. (1989) where they found that in a cell-free system the contents of late endosomes are transferred to high-density lysosomes with kinetics which are compatible with a first-order process $T_{\frac{1}{2}} \approx 5$ min. Gruenberg and Howell (1987) showed

that fusion competence of the endosomes decreased exponentially with a $T_{\frac{1}{2}} \approx 3$ min for fractions isolated 5, 15 and 30 min after internalization. However, these results do not represent the fusion competence of defined endosomal fractions but rather the vesicular trafficking of non-fusogenic late endosomes to the lysosomes, cf FIG. 3.1.2.

Disagreement with a progressive vesicular processing event, supported by Storrie et al. (1984) and Roederer et al. (1990), is based on the following: Firstly, FIG. 3.1.1 would have reflected a sigmoidal curve for the delivery of a ligand to lysosomes; Secondly the products of a maturation process cannot accumulate by first order kinetics, therefore a vesicular traffic process is believed to be involved in the delivery of a mature endosome/pre-lysosomal organelle to the lysosomes.

Control experiments

The next part of the discussion will focus on experiments that were performed to affect processing along the endocytic pathway. Firstly, the two fluid-phase markers, HRP and FITC-D, were not simply interchangeable and the concentration of HRP was critical for this experimental approach.

FIG.'s 2.1.1 (B) and 2.1.2 show the delivery of FITC-D to HRP-containing endosomes at HRP concentrations of 1 mg and 50 μg respectively. The extent of intermingling, as

represented by FITC-D solubility, was found to be dependent upon HRP concentration due to the non-linear dose-response curve (FIG. 1.2.1.). The small amount of FITC-D initially delivered into the HRP-containing endosomes could only be detected as an accordingly small fraction of FITC-D becoming insoluble. Thus, the intermingling of the fluid phase markers in FIG's 2.1.1. (B) and 2.1.2. occurred gradually over a longer time period when compared to FIG. 2.1.1 (A) where HRP was delivered to FITC-D-containing endosomes. In addition the profile depicting the experimental results for 50 μg/ml HRP in FIG. 2.1.2 (solid line) was unexpected when compared to the predicted profile (FIG. 2.1.2, dashed line) which was based on the results obtained in FIG. 2.1.1 (B) for 1 mg/ml of HRP.

FIG.'S 3.2.1 and 3.2.2 (representing the delivery of HRP to FITC-D containing lysosomes and FITC-D to HRP containing lysosomes, respectively) indicate that delivery of a ligand to the lysosomes occurs with first-order kinetics but their half-lives differ considerably, 12 and 4 min, respectively. The decrease in FITC-D solubility when HRP is delivered to FITC-D-containing lysosomes depends both on the delivery of HRP and the rate limiting interlysosomal spreading of HRP. Reversing the order of the two markers allows for the direct measurement of the decrease in FITC-D solubility when FITC-D is delivered to HRP-containing lysosomes.

Secondly, studies by Ajioka and Kaplan (1986) were undertaken at low temperature to slow the rapid cycling events to achieve a better resolution in time. Dunn *et al.* (1980); Stoscheck and Carpenter (1984); Hopkins and Trowbridge (1983); Pesonen *et al.* (1984) and Roederer *et al.* (1987 and 1990) established that endosome-lysosome fusion did not occur at low temperature. Experiments in this study were repeated at 27°C or 16°C to establish correspondence with this earlier work. The results are given as follows: maturation of endosomes at 27°C took twice as long, ≈ 8 min, when compared to similar studies at 37°C and endosome-lysosome fusion did occur at 16°C following an incubation period of 5 h (as previously found by Haylett and Thilo, 1991). The incubation period for the previously performed experiments was insufficient and intermingling at temperatures below 20°C was not observed.

Thirdly, Na^+ depletion has been reported by Baenziger and Fiete (1982); Wolkoff *et al.* (1984) and Ward *et al.* (1990) to inhibit delivery of ligands to lysosomes. Similarly, as a control for inhibition of lysosomal delivery of HRP in this study, cells were incubated in isotonic K^+ buffer prior to HRP uptake (FIG. 3.2.1). Delivery of HRP to lysosomes appeared to be inhibited, however it was not known whether HRP was initially endocytosed by the cells.

Thus to establish whether endocytosis of a ligand occurs in the presence of a Na^+-depleted buffer, FITC-D was used as a ligand and the fluorescence measured. FITC-D was endocytosed and delivered to the lysosomes, $T_{\frac{1}{2}} \approx 8$ min, hence contradicting the results in FIG. 4.1.1 and previous reports. Another method could have been used at this stage, ie. an HRP assay performed on the samples in FIG. 3.2.1 to confirm that HRP uptake initially occurred (assay not undertaken at the time of experiment). However, a Na^+-depleted buffer did inhibit lysosomal delivery and thus further investigations regarding this issue would not have been pursued. At a closer look at the results in FIG. 3.2.1, there is a tendency, by the final three samples (O), towards a lower FITC-D solubility thus implying delivery of HRP to lysosomes.

Percoll gradients were used to isolate the lysosomes from the less dense fractions to study the delivery of a ligand to lysosomes in the presence of a Na^+-depleted buffer. Na^+ depletion was found to cause a shift in the lysosomal density towards a lower density region (FIG. 4.2.4). The change in lysosomal density together with the decreased rate of HRP delivery to lysosomes (FIG. 4.2.3), compared to Na^+-containing buffers, is assumed to be related to the presence of a Na^+-depleted buffer.

Fourthly, during the initial stages of this study, it was anticipated that BFA could be used in later experiments as a control for the lack of intermingling or delivery to lysosomes. This was based on previous findings that BFA has profound effects on the morphology of various compartments of the endosome-lysosome system (Klausner et al., 1992 and Wood and Brown, 1992). Preliminary experiments were undertaken and showed that BFA caused a decrease in the fluid-phase uptake rates. Once BFA was removed from the medium, the cells regained normal fluid-phase uptake rates (FIG'S. 4.3.1 and 4.3.2).

It would have been preferable to compare the results in this study with results obtained from another cell line. An attempt was made using CHO-cells obtained from this department. This was unsuccessful as uptake appeared to be very slow and the technique employed was cumbersome when using petri-dishes. The need for a reliable and efficient protocol was evident and due to time constraints I did not pursue the matter further.

A model for organellar processing

In conclusion, the findings in this study in terms of a kinetic analysis of endosome processing can be summarized as follows: early endosomes undergo a process of maturation, as depicted by a sigmoidal curve for the intermingling of sequentially endocytosed ligands, to become non-fusogenic

late endosomes with a maturation time of 3 minutes; further delivery of a ligand from the late non-fusogenic endosomes to the lysosomes occurs by vesicular traffic where the ligands are seen to appear in high density lysosomes by random delivery and accumulate with first-order kinetics, $T_{\frac{1}{2}}$ ≈ 5 minutes.

MATERIALS AND METHODS

(i) Cell culture

Cells of the mouse macrophage cell line, $P388D_1$ (Koren *et al.*, 1975), were cultivated as previously described by Haylett and Thilo (1986). Cells were grown into suspension from a confluent monolayer and after a growth period of not longer than 24 h in fresh medium (RPMI, 10% Fetal Calf Serum (FCS), 100 U/ml penicillin and streptomycin, buffered in 5% CO_2 atmosphere). Cells were collected from suspension by centrifugation (1000 rpm, 5 min, 4°C) and washed twice with 4-[2-hydroxyethyl]-1-piperazine-ethane-sulphonic acid (Hepes)-saline buffer (HSB): 10 mM Hepes, 140 mM NaCl, pH 7.4, 1 mg/ml Bovine Serum Albumin (BSA: Fraction V, lyophilized, MW 40200) on ice. For a typical experiment, 80 - 120 x 10^6 cells were used, with a viability of 95-98% as observed via trypan-blue exclusion. Hepes and BSA obtained from Boehringer Mannheim.

(ii) Endocytosis of fluid-phase markers

Cells were incubated at about 5 x 10^6 cells/ml in hepes-buffered RPMI-medium, 1% BSA, in an Erlenmeyer flask (size 100 ml) with gentle rotatory agitation in a waterbath at 37°C. Fluid-phase markers were predissolved at 20-fold final concentration and added at 3 mg/ml for FITC-D (MW 71200, 0.005 mol/mol glucose; Sigma) and/or at the indicated concentration for HRP (MW 40200, 250 U/mg; Seravac S.A.) in

the presence of mannan (yeast, 1 mg/ml; Sigma). When a rapid warming step from ice to 37°C was required, a concentrated cell suspension in cold medium was diluted 1:5 into prewarmed medium. Endocytic uptake was stopped by cooling by 1:5 dilution into ice-cold HSB, followed by 3 washing steps by centrifugation in the same volume and using fresh centrifugation tubes after the second washing step. Where required, cell concentration was determined by Coulter-counting after the washing procedure.

(iii) DAB-crosslinking in whole cells and solubilization

Accumulation of polymerized DAB (MW 214.3, free base; Sigma) inside HRP-containing organelles induces a major increase in their equilibrium density, while other organelles of the same fraction are essentially unaffected. In those vesicles that contain HRP, DAB is oxidized and polymerized in the presence of H_2O_2 and remains trapped (Courtoy *et al.*, 1984).

Samples of about 2 - 3 x 10^6 cells, containing FITC-D in combination with HRP, were resuspended in 1 ml hepes saline (HS) (i.e. no BSA) on ice. DAB solution was freshly prepared at 3 mg/ml in HS and filtered through 0.22 μ Millipore filter. 180 μl of DAB solution was added to the cell suspension which was then incubated in the dark for 30 min on ice with occasional agitation to allow the diffusion of DAB into the cells without displacing the intracellular distribution of the two endocytosed markers. H_2O_2 was then

added to a final concentration of 0.005% (20 μl of a 0.3% solution), the solution warmed to room temperature in a water bath and incubated for 20 min in the dark to allow the H_2O_2 to diffuse into the cell and polymerize the DAB within the HRP-containing organelles. The reaction was stopped by the addition of 4 ml HSB at room temperature. Cells were pelleted and resuspended in 1 ml HS. 100 μl was then used to measure cell concentration by coulter-counting (after which samples could be stored at 4°C, overnight). 600 μl HS was added to give a total volume of 1.5 ml (at least 1 ml was required to sufficiently fill the cuvette for fluorescence measurement). Triton X-100 (Sigma) was added to a final concentration of 1% (100 μl of a 20% solution). Deoxyribonuclease (DNase) (3000 U/mg; Seravac S.A.) was added to a final concentration of 0.3 mg/ml (40 μl of a 15 mg/ml solution). Samples were incubated at 37°C for 15 min with occasional shaking. After solubilization, samples were transferred into Eppendorf tubes (1.5 ml) and centrifuged for 10 min at 20 000 x g. 1 ml was collected from the top and was used for measuring fluorescence intensity. Samples for full solubility were obtained by omitting HRP, H_2O_2 or DAB, in all cases with the same result (about 90% solubility).

(iv) Measurement of fluorescence intensity

Cells were solubilized in 0.2% triton X-100 and DNase, then centrifuged to remove debris. Fluorescence was measured in a

1 ml cuvette using a Perkin-Elmer fluorescence spectrophotometer type 203, with excitation at 470 nm and emission at 515 nm. In view of the rather low fluorescence intensities to be detected, care had to be taken that the fluorescence signal was properly resolved from the light-scattering peak. FIG. 1.3.1 illustrated typical spectras for the present conditions. The instrument was set to zero against 1 ml HS. Then, sensitivity was selected to give a full-scale reading for the most intensely fluorescing sample of a series. All other samples within the series were measured at the same setting.

(v) Subcellular fractionation

A 27% Percoll gradient was required to isolate early and late endosomes from the lysosomes (Haylett and Thilo, 1986 and 1991). Using a plastic centrifuge tube, percoll (37.8 ml) in 7.3mM Hepes, 0.18M sucrose, 0.73M ethylenediaminetetraacetic acid (EDTA) homogenizing buffer (HB) (pH 7.4)(102.2 ml) was pipetted onto a 0.5 ml cushion of 2.5M sucrose. Cells were pelleted and resuspended in HB on ice, transferred to a syringe and placed in a cell cracker; after homogenization the samples were pelleted by centrifugation (2000 rpm, 10 min). The samples were gently layered onto the percoll gradient and the tubes were spun at 25 000 x g for 90 min in a Beckman ultracentrifuge using an SW-40 rotor at 4°C. The gradients were then fractionated by piercing the bottom of the tubes with a needle and allowing

0.5 ml aliquots of the solution to run, by gravity, into 24 tubes assembled in a LKB Bromma 2112 Redirac fraction collector. The weight of each fraction had to be determined in order to determine their densities. Due to a shallow middle part of the gradient, at density of about 1.07 g/cm^3 (Haylett and Thilo, 1991), the population of lysosomes was divided into a more dense and less dense fraction. Recovery of lysosomal marker-enzyme (hexosaminidase) in the high-density fractions was about 50%. This value was used to normalize the fraction of endocytic marker (FITC-D, HRP) in terms of lysosomal delivery. Organelle breakage due to cell fractionation was less than 20%.

(vi) HRP Assay

The enzymatic activity of HRP was determined by the method of Steinman *et al.* (1976). The substrate solution for the assay was made by adding solution B (20 mM citric acid, 150 mM NaCl) to solution A (20 mM Na_2HPO_4, 110mM NaCl) until the pH was 4.30. Into this buffer was added 0.55 μg/ml 2,2'-azino-di-[3-ethylbenthiazolinesulfonate] (ABTS) (Boehringer Mannheim), 0.003% H_2O_2 and 0.2% triton X-100.

For density gradient fractions a 0.5 ml aliquot of substrate solution was added to 50 μl of each fraction from the density gradient. This was incubated at room temperature for 10 min. A 0.5 ml aliquot of `stopping solution' (100 mM citric acid, 0.01% NaN_3) was added and the absorbance was

measured at 420 nm after centrifuging the samples at low speed to remove acid precipitable protein.

(vii) NAGA Assay

To assay for ß-N-acetylaminodeoxyglucosidase the following solutions were first prepared. The substrate buffer contained 50 mM citric acid, tritrated to pH 5.0 with NaOH. A substrate solution containing 4 mM p-nitrophenyl-ß-N acetylamino deoxyglucoside was then added to the substrate buffer. Triton X-100 (20%), 100 µl/10 ml, was then finally added to this substrate solution. For the stopping buffer a 50 mM NaOH solution was required.

The assay required a 20 µl sample which was placed in an Eppendorf tube on ice. A 200 µl substrate solution was added and the samples were incubated for 30 min at 37°C using a waterbath. To stop the reaction the samples were placed on ice, 800 µliter stopping buffer was added to each sample, and the absorbance measured at 400 nm using a Unicam spectrophotometer.

(viii) Modified medium containing either Na^+ or K^+

The composition of the modified mediums were prepared as follows: NaCl or KCl 0.132 M; NaH_2PO_4 or KH_2PO_4 0.59 mM; Na_2HPO_4 or K_2HPO_4 2.12 mM; $MgCl_2$ 1.2 mM; $MgSO_4$ 0.81 mM; glucose 27.8 mM; $CaCl_2$ 2.5 mM and hepes 25 mM (Wolkoff *et al.*, 1984).

Na^+ and K^+ buffers were prepared separately. For a Na^+/K^+ buffer, equal volumes of both buffers were added together and for a Na^+-depleted buffer, K^+ buffer solely used.

(ix) Brefeldin A (BFA)

A stock solution of BFA (Sigma, 10 mg/ml in methanol) was diluted in buffer to give a 10 μg/ml solution.

ABBREVIATIONS USED

ABTS: 2,2'-azino-di-[3-äthylbenthiazolinsulfonate]

ATP: Adenosine 5'-triphosphate

BFA: Brefeldin A

BSA: Bovine serum albumin

cf: refer to

CHO: Chinese hamster ovary

CURL: Compartment for uncoupling of receptor and ligand

DAB: 3,3'-diaminobenzidine

DNase: Deoxyribonuclease

EDTA: ethylenediamine-tetraacetic acid

ER: Endoplasmic reticulum

FCS: Fetal calf serum

FI: Fluorescence intensity

FIG: Figure

FITC-D: fluoresceine isothiocyanate-dextran

h: hour

Hepes: 4-[2-Hydroxyethyl]-1-piperazin-ethan-sulfonsäure

HB: Homogenizing buffer

HRP: horse radish peroxidase

HS: hepes saline

HSB: hepes saline buffer

min: minutes

NAGA: ß-N-acetylaminodeoxyglucosidase

PNS: Post-nuclear supernatant

RER: Rough endoplasmic reticulum

t: time

$T_{\frac{1}{2}}$: half-life

Tf-HRP: HRP conjugated to transferrin

TGN: Trans-golgi network

REFERENCES

Ajioka, R. S. and Kaplan, J. 1986. Intracellular pools of transferrin receptors result from constitutive internalization of unoccupied receptors. *Proc. Natl. Acad. Sci. U.S.A.* 83: 6445-6449.

Baenziger, J. U. and Fiete, D. 1982. Recycling of the hepatocytic asialoglycoprotein receptor does not require delivery of ligand to lysosomes. *J. Biol. Chem.* 257: 6007-6009.

Begg, M. J. (1992) MSc. Thesis: The effect of hyperosmolarity on fluid-phase and receptor-mediated endocytosis in $P388D_1$ macrophages. University of Cape Town, Medical Biochemistry.

Braell, W. A. 1987. Fusion between endocytic vesicles in a cell-free system. *Proc. Natl. Acad. Sci. U.S.A.* 84: 1137-1141.

Courtoy, P. J., Quintart, J. and Baudhuin, P. 1984. Shift of equilibrium density induced by 3,3'-Diaminobenzidine cytochemistry: A new procedure for the analysis and purification of peroxidase-containing organelles. *J. Cell Biol.* 98: 870-876.

Davey, J., Hurtly, S. M. and Warren, G. 1985. Reconstitution of an endocytic fusion event in a cell-free system. *Cell* 43: 643-652.

Davoust, J., Gruenberg, J. and Howell, K. 1987. The threshold values of low pH block endocytosis at different stages. *EMBO J.* 6: 3601-3609.

De Duve, C. and Wattiaux, R. 1966. Functions of lysosomes. *Ann. Rev. of Physiol.* 28: 435-492.

Diaz, R., Mayorga, L. and Stahl, P. 1988. *In vitro* fusion of endosomes following receptor-mediated endocytosis. *J. Biol. Chem.* 263: 6093-6100.

Dunn, W. A., Hubbard, A. L. and Aronson, N. N., Jr. 1980. Low temperature selectivity inhibits fusion between pinocytic vesicles and lysosomes during heterophagy of I^{125}-Asialofetuin by perfused rat liver. *J. Biol. Chem.* 255: 5971-5978.

Dunn, K. W. and Maxfield, F. R. 1992. Delivery of ligands from sorting endosomes to late endosomes occurs by maturation of sorting endosomes. *J. Cell Biol.* 117: 301-310.

Ferris, A. L., Brown, J. C., Park, R. D. and Storrie, B. 1987. Chinese Hamster Ovary cell lysosomes rapidly exchange contents. *J. Cell Biol.* 105: 2703-2712.

Geuze, H. J., Slot, J. W. and Strous, G. J., Lodish, H. F. and Schwartz, A. C. 1983. Intracellular site of asialoglycoprotein receptor-ligand uncoupling: Double-label immunoelectron microscopy during receptor-mediated endocytosis. *Cell* 32: 277-287.

Geuze, H. J., Stoorvogel, W., Strous, G. J., Slot, J. W., Bleekemolen, J. E. and Mellman, I. 1988. Sorting of

mannose 6-phosphate receptors and lysosomal membrane proteins in endocytic vesicles. *J. Cell Biol.* 107: 2491-2501.

Griffiths, G. and Gruenberg, J. 1991. The arguments for pre-existing early and late endosomes. *Trends in Cell Biol.* 1: 5-9.

Gruenberg, J. E. and Howell, K. E. 1986. Reconstitution of vesicle fusions occuring in endocytosis with a cell-free sysytem. *EMBO J.* 5: 3091-3101.

Gruenberg, J. E. and Howell, K. E. 1987. An internalized transmembrane protein resides in a fusion-competent endosome for less than 5 minutes. *Proc. Natl. Acad. Sci. U. S. A.* 84: 5758-5762.

Gruenberg, J. E. and Howell, K. E. 1989. Membrane traffic in endocytosis: Insights from cell-free assays. *Annu. Rev. Cell Biol.* 5: 453-481.

Gruenberg, J. E., Griffiths, G. and Howell, K. E. 1989. Characterization of the early endosome and putative endocytic carrier vesicles *in vivo* and with an assay of vesicle fusion *in vitro*. *J. Cell Biol.* 108: 1301-1316.

Haylett, T. and Thilo, L. 1986. Limited and selected transfer of plamsma membrane glycoproteins to membrane of secondary lysosomes. *J. Cell Biol.* 103: 1249-1256.

Haylett, T. and Thilo, L. 1991. Endosome-lysosome fusion at low temperature. *J. Biol. Chem.* 266: 8322-8327.

Hopkins, C. R., Gibson, A., Shipman, M. and Miller, K. 1990. Movement of internalized ligand-receptor complexes along a continuous endosomal reticulum. *Nature* 346: 335-339.

Hopkins, C. R. and Trowbridge, I. S. 1983. Internalization and processing of the transferrin receptor in human carcinoma A431 cells. *J. Cell Biol.* 97: 508-521.

Hunziker, W., Whitney, J. A. and Mellman, I. 1992. Brefeldin A and the endocytic pathway: Possible implications for membrane traffic and sorting. *FEBS Lett.* 307: 93-96.

Klausner, R. D., Donalson, J. G. and Lippincott-Schwartz, J. 1992. Brefeldin A: Insights into the control of membrane traffic and organelle structure. *J. Cell Biol.* 116: 1071-1080.

Koren, H. S., Handwerger, B. S. and Wunderlich, J. R. 1975. Identification of macrophage-like characteristics in a cultured Murine Tumour line. *J. Immunol.* 114: 894-897.

Lippincott-Schwartz, J., Yuan, L., Tipper, C., Amherdt, M., Orci, L. and Klausner, R. D. 1991. Brefeldin A's effects on endosomes, lysosomes and the TGN suggest a general mechanism for the regulating organelle structure and membrane traffic. *Cell* 67: 601-616.

Marsh, M., Bolzau, E. and Helenius, A. 1983. Penetration of Semliki Forest Virus from acidic prelysosomal vacuoles. *Cell* 32: 931-940.

Marsh, M., Griffiths, G., Dean, G. E., Mellman, I. and Helenius, A. 1986. Three-dimensional structure of

endosomes in BHK-21 cells. *Proc. Natl. Acad. Sci. U. S. A.* 83: 2899-2903.

Mayora, L. S., Diaz, R. and Stahl, P. D. 1988. Plasma membrane-derived vesicles containing receptor-ligand complexes are fusogenic with early endosomes in a cell-free sysytem. *J. Biol. Chem.* 263: 17213-17216.

Mellman, I. S., Steinman, R. M., Unkless, J. C. and Cohn, Z. A. 1980. Selective Iodination of polypeptide composition of pinocytic vesicles. *J. Cell Biol.* 86: 712-722.

Merion, M. and Sly, W. S. 1983. The role of intermediate vesicles in the adsorptive endocytosis and transport of ligand to lysosomes by Human Fibroblasts. *J Cell Biol.* 96: 644-650.

Misumi, Y., Miki, K., Takatsuki, A., Tamura, G. and Ikehara, Y. 1986. Novel blockade by Brefeldin A of intracellular transport of secretory proteins in cultured Rat Hepatocytes. *J. Biol. Chem.* 261: 11398-11403.

Mueller, S. C. and Hubbard, A. L. 1986. Receptor-mediated endocytosis of asialoglycoproteins by Rat Hepatocytes: Receptor-positive and receptor negative endosomes. *J. Cell Biol.* 102: 932-942.

Mullock, B. M., Branch, W. J., van Schaik, M., Gilbert, L. K. and Luzio, J. P. 1989. Reconstitution of an endosome-lysosome interaction in a cell-free sysytem. *J. Cell Biol.* 108: 2093-2099.

Murphy, R. F. 1985. Analysisis and isolation of endocytic vesicles by flow cytometry and sorting: Demonstration of

three kinetically distinct compartments involved in fluid-phase endocytosis. *Proc. Natl. Acad. Sci. U. S. A.* 82: 8523-8526.

Palade, G. 1975. Intracellular aspects of the process of protein sysnthesis. *Science* 189: 347-385.

Pearse, B. M. F. and Bretscher, M. S. 1981. Membrane recycling by coated vesicles. *Ann. Rev. Biochem.* 50: 85-101.

Pelham, H. R. B. 1991. Multiple targets for Brefeldin A. *Cell* 67: 449-451.

Pesonen, M., Ansorge, W. and Simons, K. 1984. Transcytosis of the G Protein of Vesicular Somatitis Virus after implantation into the apical plasma membrane of Madin-Darby Canine Kidney cells. 1. Involvement of endosomes and lysosomes. *J. Cell Biol.* 99: 796-802.

Racoosin, E. L. and Swanson, J. A. 1993. Macropinosome maturation and fusion with tubular lysosomes in macrophages. *J. Cell Biol.* 121: 1011-1020.

Roederer, M., Barry, J. R., Wilson, R. B. and Murphy, R. F. 1990. Endosomes can undergo and ATP-dependent density increase in the absence of dense lysosomes. *Eur. J. Cell. Biol.* 51: 229-234.

Roederer, M., Bowser, R. and Murphy, R. F. 1987. Kinetics and temperature dependence of exposure of endocytosed material to proteolytic enzymes and low pH: Evidence for a maturation model for the formation of lysosomes. *J. Cell. Phys.* 131: 200-209.

Salzman, N. H. and Maxfield, F. R. 1988. Intracellular fusion of sequentially formed endocytic compartments. *J. Cell Biol.* 106: 1083-1091.

Salzman. N. H. and Maxfield, F. R. 1989. Fusion accessibility of endocytic compartments along the recycling and lysosomal endocytic pathways in intact cells. *J. Cell Biol.* 109: 2097-2104.

Samuelson, A. C., Stockert, R. J., Novikoff, A. B., Novikoff, P. M., Saez, J. C. and Wolkoff, A. W. 1988. Infuence of cytosolic pH on receptor-mediated endocytosis. *Am. J. Physiol.* 254: C829-838.

Schlossman, D. M., Schmid, S. L., Braell, W. A. and Rothman, J. E. 1984. An enzyme that removes clathrin coats: Purification of an uncoating ATPase. *J. Cell Biol.* 99: 723-734.

Schmid, S. L., Fuchs, R., Male, P. and Mellman, I. 1988. Two distinct subpopulations of endosomes involved in membrane recycling and transport to lysosomes. *Cell* 52: 73-83.

Silverstein, S. C., Steinman, R. M. and Cohn, Z. A. 1977. Endocytosis. *Ann. Rev. Biochem.* 46: 669-722.

Stahl, P. D. and Gordon, S. 1982. Expression of a Mannosyl-Fucosyl Receptor for endocytosis on cultured Primary Macrophages and their hybrids. *J. Cell Biol.* 93: 49-56

Steinman, R. M. and Cohn, Z. A. 1972. The interaction of soluble Horseradish Peroxidase with Mouse peritoneal Macrophages *in vitro*. *J. Cell Biol.* 55: 186-204.

Steinman, R. M., Brodie, S. E. and Cohn, Y. A. 1976. Membrane flow during pinocytosis: A stereologic analysis. *J. Cell Biol.* 68: 665-687.

Steinman, R. M., Mellman, I. S., Muller, W. A. and Cohn, Z. A. 1983. Endocytosis and the recycling of plasma membrane. *J. Cell Biol.* 96: 1-27.

Stoorvogel, W., Strous, G. J., Geuze, H. J., Oorschot, V. and Schwartz, A. L. 1991. Late endosomes derive from early endosomes by maturation. *Cell* 65: 417-427.

Storrie, B., Pool, R. R., Sachdeva, M., Maurey, K. M. and Oliver, C. 1984. Evidence for both prelysosomal and lysosomal intermediates in endocytic pathways. *J. Cell Biol.* 98: 108-115.

Stoscheck, C. M. and Carpenter, G. 1984. Down regulation of epidermal growth factors receptors: Direct demonstration of receptor degradation in Human Fibroblasts. *J. Cell Biol.* 98: 1048-1053.

Straus, W. 1964. Occurance of phagosomes and phago-lysosomes in different segments of the nephron in relation to the reabsorption, transport, digestion and extrusion of intravenously injected Horseradish Peroxidase. *J. Cell Biol.* 21: 295-308.

Swanson, J. A., Yirinec, B. D. and Silverstein, S. C. 1985. Phorbol esters and Horseradish Peroxidase stimulate pinocytosis and redirect the flow of pinocytosed fluid in macrophages. *J. Cell Biol.* 100: 851-859.

Tolleshaug, H., Berg, T., Fröhlich, W. and Norum, K. R. 1979. Intacellular localization and degradation of asialofetuin in isolated Rat Hepatocytes. *Biochem. Biophys. Acta*. 585: 71-84.

Tooze, J. and Hollinshead, M. 1991. Tubular early endosomes networks in AtT20 and other cells. *J. Cell Biol*. 115: 635-653.

Wall, D. A. and Hubbard, A. L. 1984. Receptor-mediated endocytosis of Asialoglycoproteins by Rat Liver Hepatocytes: Biochemical characterization of the endosomal compartments. *J. Cell Biol*. 101: 2104-2112.

Wall, D. A., Wilson, G. and Hubbard, A. L. 1980. The galactose-specific recognition system of mamalian liver: the route of ligand internalization in Rat Hepatocytes. *Cell* 21: 79-93.

Ward, D. M., Ajioka, R. and Kaplan, J. 1989. Cohort movement of different ligands and receptors in the intracellular endocytic pathway of alveolar macrophages. *J. Biol. Chem*. 264: 8164-8170.

Ward, D. M., Hackenyos, D. P. and Kaplan, J. 1990. Fusion of sequentially internalized vesicles in Alveolar Macrophages. *J. Cell Biol*. 110: 1013-1022.

Wileman, T. E., Lennartz, M. R. and Stahl, P. D. 1986. Identification of the macrophage mannose receptor as a 175-kDa membrane protein. *Proc. Natl. Acad. Sci. U. S. A*. 83: 2501-2505.

Wolkoff, A. W., Klausner, R. D., Ashwell, G. and Harford, J. 1984. Intracellular segregation of Asialoglycoproteins and their receptor: A prelysosomal event subsequent to dissociation of the ligand-receptor complex. *J. Cell Biol.* 98: 375-381.

Wood, S. A. and Brown, W. J. 1992. The morphology but not the function of endosomes and lysosomes is altered by Brefeldin A. *J. Cell Biol.* 119: 273-285.

Wood, S. A., Park, J. E. and Brown, W. J. 1991. Brefeldin A causes a microtubule-mediated fusion of the trans-golgi network and early endosomes. *Cell* 67: 591-600.

Woodman, P. G. and Warren, G. 1988. Fusion between the vesicles from the pathway of receptor-mediated endocytosis in a cell-free system. *Eur. J. Biochem.* 173: 101-108.